Supplementary Information

Ultrasensitive regulation of anapleurosis via allosteric activation of PEP carboxylase

Yi-Fan Xu[1,2], Daniel Amador-Noguez[1], Marshall Louis Reaves[1,3], Xiao-Jiang Feng[2], Joshua D. Rabinowitz[1,2,*]

[1]Lewis Sigler Institute for Integrative Genomics, Princeton University, Princeton, NJ 08544, USA. [2]Department of Chemistry, Princeton University, Princeton, NJ 08544, USA. [3]Department of Molecular Biology, Princeton University, Princeton, NJ 08544, USA

*To whom correspondence should be addressed. E-mail: joshr@princeton.edu

Supplementary Methods

Culture conditions and metabolite extraction.

Detailed protocols for preparing filter cultures and extracting metabolites in *Escherichia coli* have been published[1,2]. Briefly, *E. coli* K-12 strain NCM3722 was grown at 37°C in minimal salts media[3] with 10 mM ammonium chloride as the nitrogen source and 0.4% (w/v) glucose as the carbon source. To obtain exponential-phase cultures, saturated overnight cultures were diluted 1:30 and then grown in liquid media in a shaking flask to A600 (absorbance at 600 nm) of ~ 0.1. A portion of the cells (1.6 mL) was then transferred to nylon membrane filters (Millipore) resting on vacuum filter support. Once the cells were loaded, the membrane filters were transferred to media-loaded agarose plates. To measure growth, filters were washed thoroughly with 1.6 mL fresh medium and A600 determined. For metabolomics experiments, cells were grown to A600 of ~ 0.4 prior to initiation of experimental manipulations (e.g., glucose removal) and quenching of metabolism. Metabolism was quenched by direct and immediate transfer of the filters into – 20 °C extraction solvent (40:40:20 acetonitrile/methanol/water with 0.1 M formic acid to quantify nucleotide triphosphates and coenzymes, and without formic acid to quantify other metabolites[4]), and serial extraction was carried out as described previously[2]. For glucose removal, filters were then switched from glucose plates to plates containing no carbon source, 0.4% (w/v) acetate, 0.4% (w/v) succinate, or 0.4% (w/v) glycerol as the carbon source, and extracted at 1, 2, 5, 10, 20, 30, 60, 90, 120 min after the switch. Control experiments in which to cells were switched to a glucose-free plate at t = 0, and again to a new glucose-free plate at t = 1 min in the case that the first transfer did not eliminate all glucose, showed identical results to the single transfer (note that for yeast grown in 2% glucose, a single filter transfer is insufficient to remove all glucose). For experiments involving recombinant enzyme expression, an appropriate concentration of IPTG was added in both liquid media and agarose plates.

Metabolite and flux measurement.

Cell extracts were analyzed by reversed phase ion-pairing liquid chromatography (LC) coupled by electrospray ionization (ESI) (negative mode) to a high-resolution, high-accuracy mass spectrometer (Exactive; Thermo Fisher) operated in full scan mode at 1 s scan time, 10^5 resolution, with compound identities verified by mass and retention time match to authenticated standard[51]. For a list of metabolites, exact masses, and retention times, see **Supplementary Table 3**. Confirmatory analysis for a subset of compounds was conducted by a different reversed phase ion-pairing LC method coupled by negative mode ESI to a Thermo TSQ Quantum triple quadrupole mass spectrometer operating in multiple reaction monitoring mode[52]. For a list of metabolites, scan events, and retention times, see **Supplementary Table 4**. All data reported in the paper is from the high-resolution LC-MS analysis; for the compounds listed in **Supplementary Table 4**, the LC-MS/MS analysis confirmed the biological trends (see **Supplementary Fig. 22** for PEP and FBP data). Absolute intracellular

metabolite concentrations in steadily growing *E. coli* were previously determined[48]. Metabolite concentrations after perturbations were computed based on fold-change in ion counts relative to steadily-growing cells (grown and analyzed in parallel) multiplied by the known absolute concentration in the steadily growing cells.

In **Fig. 1**, isomers such as F6P/G6P, GAP/DHAP, 3PG/2PG was lumped together due to similar chromatographic retention time. When separate measurements of isomeric species are reported, this is based on chromatographic resolution of the isomers.

Quantitation of PEP carboxylase

E. coli cells were grown on either glucose or acetate minimal media plates as described above. When the culture reached A600 of ~ 0.4, the cells were washed off the filter with 1.6 mL ice-cold glucose or acetate minimal liquid media and used as the steady state sample. For the 10 min carbon starvation and 10 min acetate switch samples, following transfer to the appropriate glucose-free plates for 10 min, ice-cold no carbon or acetate minimal liquid media were used to wash the cells off the filters. 25 µL cells were pelleted, re-suspended in 10 µL SDS-running buffer (Bio-Rad), and boiled for 8 minutes. Proteins were separated by SDS-PAGE on TGX 12% gels (Bio-Rad) and visualized by Coomassie staining (GelCode Blue, Pierce). The band for PEP carboxylase (indicated by the strong staining of the over-expressed enzyme) was excised, destained, and washed extensively. The sample was then subjected to in-gel thiol reduction with DTT, alkylation with iodoacetamide, and overnight trypsin digestion (Trypsin Gold, Promega)[5]. Peptides were eluted from the gel, concentrated, and reconstituted in 3% acetonitrile/0.1% formic acid. Sample concentration and desalting were performed using a trapping capillary column (150 µm x ca. 40 mm, packed with 5 µm, 100 Å Magic AQ C18 material, Michrom) at a flow rate of 5 µL/min for 3.5 min, while separation was achieved using an analytical capillary column (75 µm x ca. 12 cm, packed with 1.7 µm, 100 Å C18 BEH material, Waters), under a linear gradient of A and B buffers (buffer A: 3% acetonitrile/0.2% formic acid/0.1% acetic acid; buffer B: 97% acetonitrile/0.2% formic acid/ 0.1% acetic acid) over 60 min at a flow rate of approximately 300nL/min. Samples were analyzed by reversed-phase LC-MS performed on a nano-flow capillary high pressure HPLC system (Eksigent) coupled to a Thermo LTQ-Orbitrap mass spectrometer, outfitted with a NanoMate ion source robot (Advion). The instrument was set to operate in pseudo-SRM mode. PEP carboxylase was quantitated based on the most prominent peptide ion, the $[M+3H]^{3+}$ ion at *m/z* 405.22837, derived from the sequence AGIELTLFHGR, and its most prominent daughter ion, the $y8^{2+}$ fragment ion at *m/z* 487.06. Nanospray ionization was conducted using the NanoMate in LC-coupling mode at 1.74 kV. The NanoMate was used to feed an LTQ-Orbitrap mass spectrometer with the LTQ heated capillary at 200 ℃. Further information on mass spectrometry parameters is included in the main text.

Preparation of PEP carboxylase

E. coli PEP carboxylase was purified from bacteria that carried plasmid pCA24N (from ASKA library) that encoded His-tagged PEP carboxylase[6] using Ni-NTA spin columns (QIAGEN). The purification protocol was modified as below to obtain nearly homogenous expression of tetrameric enzyme. These modifications were based on our observation by gel filtration that excessive PEP carboxylase expression causes the formation of octamers, which are less responsive to FBP activation and aspartate inhibition. The modified protocol is as follows: a saturated overnight culture of *E. coli* containing the PPC expression plasmid and grown in glucose minimal media was diluted 1:50 into fresh glucose minimal media. After the cells reached A600 of ~0.5, IPTG was added to a final concentration of 0.2 mM and PEP carboxylase expressed for 1.5 hours. Cells were pelleted from 100 mL of culture medium and resuspended in 1 mL PBS buffer, treated with lysozyme, and lysed in a Misonix 3000 sonicator. Cell lysates (supernatants) were collected after 30 min of centrifugation at 13,000 g, and applied to Ni-NTA spin columns following protocols provided by QIAGEN. Eluate containing 200 µg/mL PEP carboxylase was collected and used for enzyme assays.

For measurement of PEP carboxylase activity in cell extracts, *E. coli* cells growing on plates were washed off the filter with ice-cold liquid media, pelleted, re-suspended in PBS buffer, treated with lysozyme, and lysed in a Misonix 3000 sonicator. The protein preparation process was carried out at 4℃.

Measurement of PEP carboxylase activity

The PEP carboxylase reaction was coupled to the malate dehydrogenase (MDH) reaction as described previously[7]. However, instead of using a spectrophotometer to measure the decrease of NADH at 340 nm, we used LC-MS to directly measure the reaction product malate. The rationale is as follows: Even purified PEP carboxylase enzyme contains contaminants which slowly oxidize NADH. Thus the decrease of NADH is not solely due to the malate dehydrogenase reaction. This becomes important when quantitating the low PEP carboxylase activity found in the low FBP conditions which are important physiologically after glucose removal. Since malate is the product of MDH reaction, it can only come from oxaloacetate in the purified enzyme system. Also, the background malate signal in purified enzyme sample before adding PEP carboxylase is almost zero, which facilitates accurate quantitation in low activity conditions. To differentiate malate produced by MDH (i.e., the product) from malate added as an enzyme inhibitor, we added 2,2,3-$^{2}D_3$-malate as the enzyme inhibitor. This is fully resolved from unlabeled malate by high resolution LC-MS. Also, U-^{13}C-aspartate was added to avoid potential formation of malate by the degradation of aspartate.

The basic reaction mixture contained, in a total volume of 0.5 mL, Tris-HCl buffer, pH 8.5, 100 mM; $MgCl_2$, 10 mM; $KHCO_3$, 10mM; NADH, 0.5 mM; malate dehydrogenase, 10 Units/mL; and PEP carboxylase, 0.1-2 µg/mL (depending on how much PEP was added). Substrate PEP and allosteric regulators acetyl-CoA, FBP,

aspartate, malate, and GTP were added at physiological concentrations based on the metabolomics experiments. Assays were carried out in 30℃ in an Eppendorf Thermomixer with mixing speed of 600 rpm. Reactions were started by adding PEP. At 1, 2, 5, 10, and 20 min thereafter, 20 µL of the reaction mixture was pipetted into 180 µL of – 20 ℃ extraction solvent (40:40:20 acetonitrile/methanol/water without acid) to quench the reaction and extract metabolites. Samples were then further diluted five-fold followed by LC-MS measurement.

For measurement of PEP carboxylase activity in cell extracts before and after glucose removal (**Supplementary Fig. 12b**), *E. coli* K-12 strain NCM3722 was grown on glucose minimal media plates as described above. When the culture reached A600 of ~ 0.4, the cells were washed off the filter with 1.6 mL ice-cold glucose minimal liquid media and used as the glucose steady state sample. Cells were then pelleted, re-suspended in 0.3 mL PBS buffer, treated with lysozyme and lysed in a Misonix 3000 sonicator. Cell lysates (supernatants) were collected after 30 min of centrifugation at 13,000 g. The whole process was carried out at 4 ℃. . For the 10 min carbon starvation and 10 min acetate switch samples, following transfer to the appropriate glucose-free plates for 10 min, ice-cold no carbon or acetate minimal liquid media were used to wash the cells off the filters. In the enzyme assays, 50 µL cell extract instead of purified enzyme was used to make 0.5 mL reaction mixture described above. 0.61 mM acetyl-CoA was added to activate the enzyme and 0.18 mM PEP was added to start the reaction.

Mutant construction and site-directed mutagenesis

The plasmid pCA24N in ASKA library containing PEP carboxylase was used as the template for site-directed mutagenesis reactions following the protocol of Quickchange Site-Directed Mutagenesis by Stratagene. The pair of primers used for substitution of amino acids was: 5'-GAACCGTATCagTATCTGATGAAAAACC-3' and 5'-CATCAGATActGATACGGTTCTGCGGC-3' to obtain the R313Q mutant (R → Q mutants at positions 144, 145, and 192 were constructed analogously but did not yield as complete desensitization to FBP as the R313Q mutant). The mutation site is described in lowercase letters. Briefly, the template plasmid was first denatured and annealed with the oligonucleotide primers containing the desired mutation. Then using the polymerase chain reaction (PCR), the primers were extended resulting in nicked circular strands. This nicked mutant plasmid was repaired in the competent cells and then transformed into the NCM3722 *ppc* deletion strain. The template plasmid was also transformed to the *ppc* deletion strain and used as the control. The resulting strains were named as: Δ*ppc*/pCA24N-*ppc* (control) and Δ*ppc*/pCA24N-*ppc*R313Q.

Metabolic Flux Analysis of wild type and Δ*pykA*/Δ*pykF* cells

To determine PEP and TCA cycle fluxes, including pyruvate kinase flux, for cells growing freely on glucose in filter cultures, metabolite labeling patterns (aspartate, PEP, valine, and xylulose-5-phosphate) were measured after feeding 1-^{13}C-glucose. These data were integrated with glucose consumption and acetate excretion rates and cell growth rates, with the combined information sufficient for steady-state flux quantitation (**Supplementary Fig. 6**). *E. coli* cells were grown on top of an agarose-media mixture containing 0.4% 1-^{13}C glucose. At A600 of ~ 0.4, cells were extracted as described above and the metabolome quantitated by LC-MS. In addition, glucose and acetate in the underlying agarose-media were measured by NMR; NMR analysis also ruled out the significant excretion of other metabolites.

Steady-state fluxes were fit to a reduced TCA cycle flux model which omits malic enzyme and PEP carboxykinase (**Supplementary Fig. 6c**). The former was omitted based on fitting the experimentally observed valine labeling pattern to a linear combination of pyruvate synthesis from PEP and from malic enzyme, and obtaining a malic enzyme contribution of zero (upper error bound < 2%; data not shown). The latter was omitted based on PEP's labeling pattern being consistent with the combined effects of glycolysis and the pentose phosphate pathway without significant gluconeogenic flux. Lack of gluconeogenic flux was confirmed by spiking labeled acetate into cells growing freely on glucose and observing rapid TCA cycle labeling but no detectable labeling of PEP or other glycolytic compounds (upper error bound < 1%; data not shown).

Fluxes into biomass, including the PEP carboxylase flux (F_{PPC}), were calculated based on growth rate from the known metabolite requirements for macromolecular synthesis. The largest route of pyruvate production from PEP is the PTS, and F_{PTS} equals the experimentally measured glucose uptake rate. Combined with the experimentally measured acetate excretion rate (F_{ACex}), these fluxes are sufficient to determine the flux from TCA cycle turning into oxaloacetate ($F_{\mathrm{TCA}\rightarrow\mathrm{OAA}}$) for the Δ*pykA*/Δ*pykF* cells by flux balancing. The ratio F_{PPC} / $F_{\mathrm{TCA}\rightarrow\mathrm{OA}}$ is also determined by the aspartate labeling pattern after feeding 1-^{13}C-glucose, and agrees within experimental error with the value determined by flux balancing (horizontal black lines in aspartate panel of **Supplementary Fig. 6a** show the calculated labeling pattern based on the F_{PPC} / $F_{\mathrm{TCA}\rightarrow\mathrm{OAA}}$ ratio from flux balancing; bars and error bars show the experimental data). Thus, for the Δ*pykA*/Δ*pykF* cells, the system is over-determined with the redundant independent data result in a single coherent flux set. For the wild type cells, the F_{PPC} / $F_{\mathrm{TCA}\rightarrow\mathrm{OAA}}$ ratio based on the aspartate labeling pattern (identical to the Δ*pykA*/Δ*pykF* cells based on the indistinguishable labeling) was used to calculate $F_{\mathrm{TCA}\rightarrow\mathrm{OAA}}$. Pyruvate kinase flux ($F_{PYK}$) can then be calculated by flux balancing, yielding a flux of 0.12 mmol/g CDW/h with a standard error of 0.62 mmol/g CDW/h. Flux error estimates were calculated based on experimental data error by standard rules for propagation of error through the addition, subtraction, and multiplication operations involved in the flux calculations.

Calculation of aspartate labeling pattern based on F_{PPC} / $F_{\mathrm{TCA}\rightarrow\mathrm{OAA}}$ ratio

The aspartate labeling pattern was calculated from the PEP labeling pattern based on the above TCA cycle model by full isotopomer balancing (**Supplementary Fig. 6b**). This requires not only knowledge of the number of labeled carbon atoms in PEP, but also positional labeling, which cannot be directly measured by LC-MS. Starting from 1-$^{13}C_1$-glucose, glycolysis makes an equal mix of unlabeled and 3-$^{13}C_1$-PEP. The oxidative pentose phosphate pathway selectively burns C1 of glucose as CO_2. This leads to excess unlabeled compared to $^{13}C_1$ PEP as observed experimentally (**Supplementary Fig. 6a**). In addition, we observed some $^{13}C_2$-PEP, which can be made through the non-oxidative pentose phosphate pathway; such activity also yields 1-$^{13}C_1$-PEP, whose abundance was determined by the amount of $^{13}C_2$-PEP and the xylulose-5-phosphate (Xu5P) labeling pattern (the ratio of non-labeled over singly + doubly-labeled Xu5P equals the ratio of 1-$^{13}C_1$ over 1,3-$^{13}C_2$ PEP).

Simplified steady-state model of glycolytic regulation

To examine the regulatory requirements for PEP to increase when glycolytic influx decreases, we used a simplified model of glycolysis as shown in **Supplementary Scheme 1**

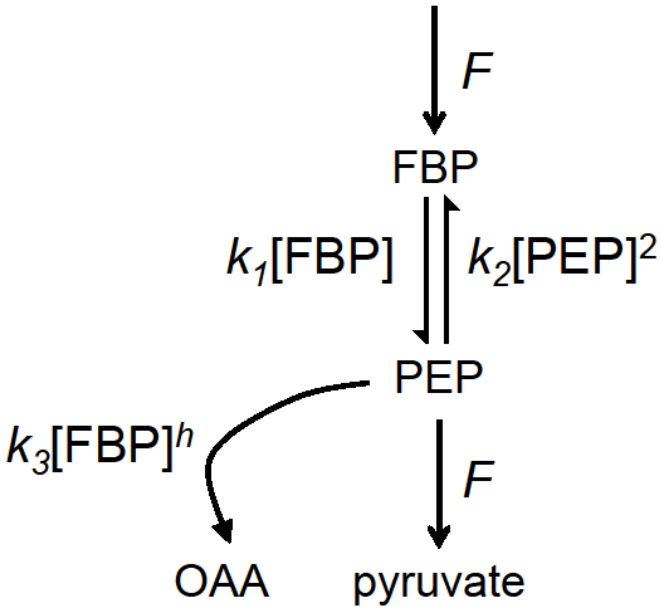

Supplementary Scheme 1

where F is the PTS flux, $k_1 - k_3$ are the rate constants of the indicated reactions, and h is the hill-coefficient for FBP activation of PEP carboxylase. Given that the bidirectional enzymes in glycolysis have large K_m, while unidirectional enzymes are saturated[9], it is reasonable to approximate the reactions between FBP and PEP as first-order, and to assume that PEP carboxylase is insensitive to [PEP]. For this simple model, the steady state kinetics of FBP and PEP are given by:

$$0 = \frac{d[\mathrm{FBP}]}{dt} = F - k_1[\mathrm{FBP}] + k_2[\mathrm{PEP}]^2$$

$$0 = \frac{d[\mathrm{PEP}]}{dt} = 2k_1[\mathrm{FBP}] - 2k_2[\mathrm{PEP}]^2 - F - k_3[\mathrm{FBP}]^h$$

These equations have a discrete solution:

$$[\mathrm{FBP}] = \left(\frac{F}{k_3}\right)^{\frac{1}{h}}$$

$$[\mathrm{PEP}] = \sqrt{\frac{k_1\left(\frac{F}{k_3}\right)^{\frac{1}{h}} - F}{k_2}}$$

In the model, when *F* decreases, [FBP] always decreases. This matches experimental observations. The qualitative behavior of PEP, however, depends on *h*. For $h = 1$, as *F* decreases, [PEP] decreases (see **Supplementary Fig. 15**). For $h < 1$, the decrease is greater. For $h > 1$, however, [PEP] can increase as *F* decreases as is experimentally observed. Thus, ultrasensitive regulation of PEP carboxylase is required to obtain the experimentally observed inverse behavior of [FBP] and [PEP].

Supplementary Results

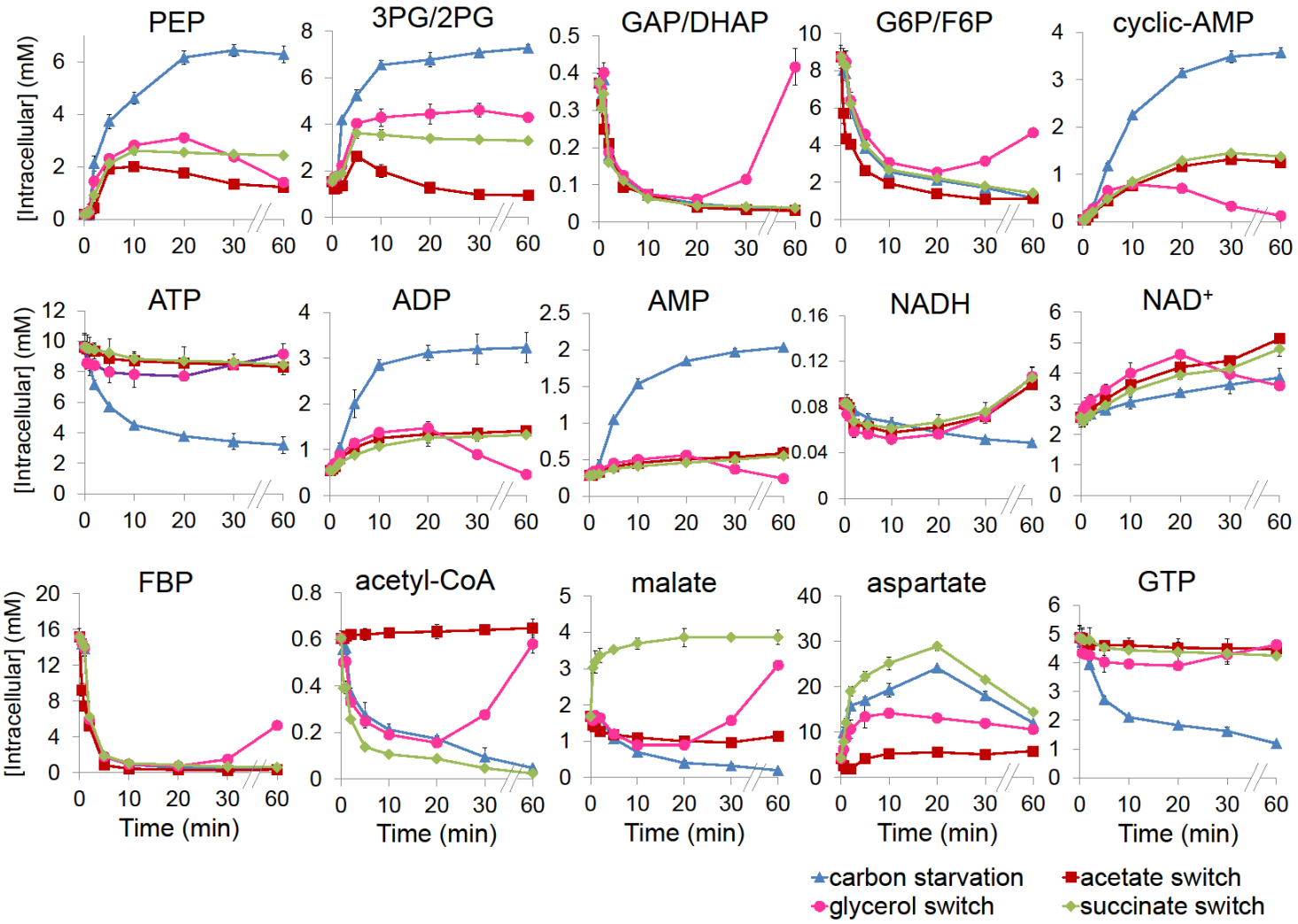

Supplementary Fig. 1. Absolute intracellular concentrations of key metabolites during glucose removal and its replacement with no carbon, acetate, succinate, or glycerol.

E. coli cells growing freely in glucose minimal media were switched to no carbon, acetate, succinate, or glycerol as indicated. After the indicated duration of glucose removal, the metabolome was quantitated by LC-MS. Cyclic-AMP spikes in all four switches, a canonical response of *E. coli* to glucose removal that activates cyclic-AMP receptor protein (CRP) to regulate the transcription of over 180 enzymes. Gluconeogenesis starts more quickly in the switch to glycerol (~ 30 min) than in the other conditions (where it takes more than 1.5 h). The *x* axis represents minutes after the switch, and the *y* axis represents absolute intracellular metabolite concentration. Points reflect data (mean ± range of N = 2 biological replicates).

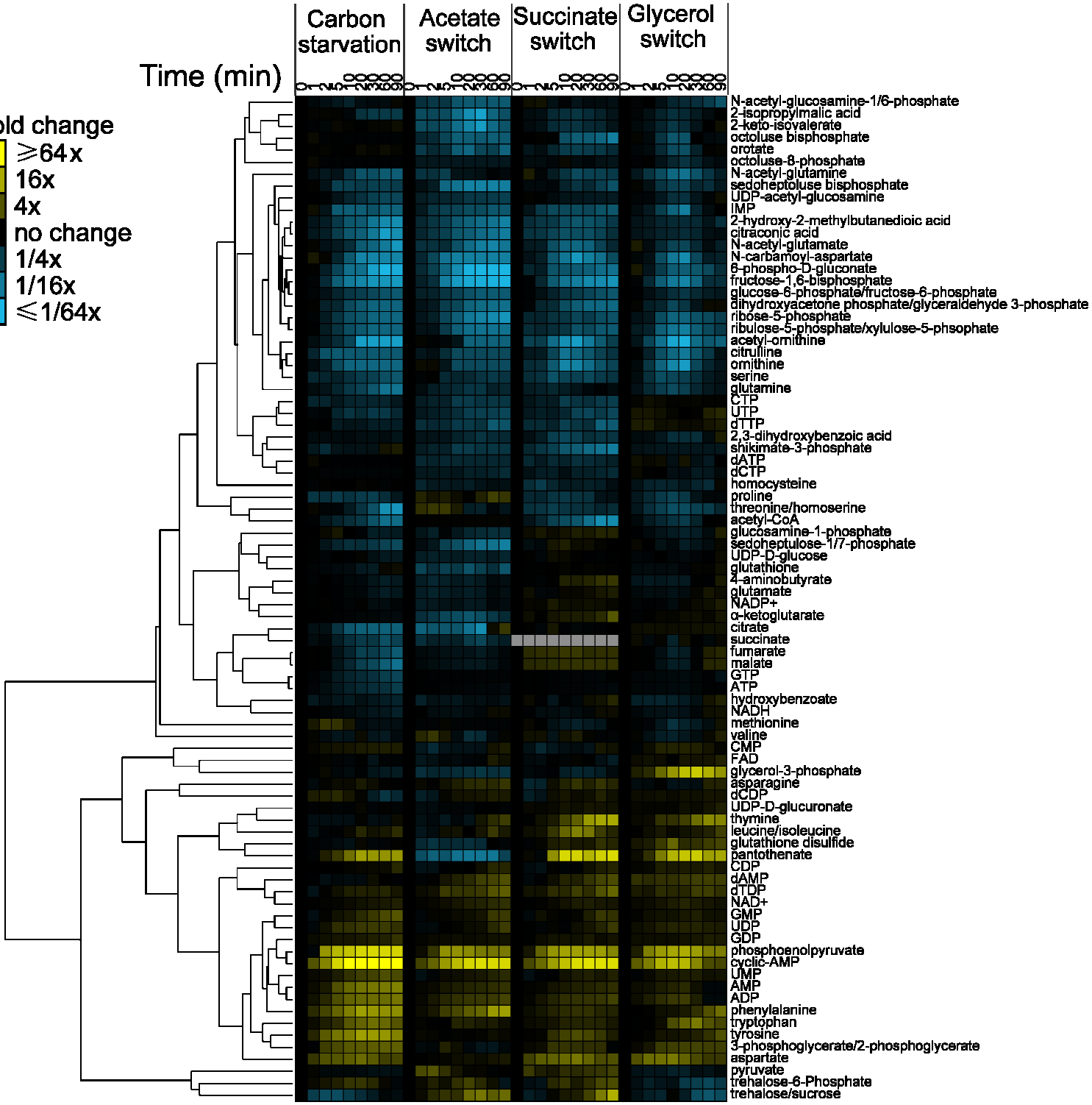

Supplementary Fig. 2. Heat map of all measured metabolites during glucose removal and its replacement with no carbon, acetate, succinate, or glycerol.

E. coli cells growing freely in glucose minimal media were switched to no carbon, acetate, succinate, or glycerol as indicated. After the indicated duration of glucose removal, the metabolome was quantitated by LC-MS. Metabolite levels of biological duplicates were averaged, normalized to cells growing steadily in glucose (time zero), and the resulting fold changes log transformed.

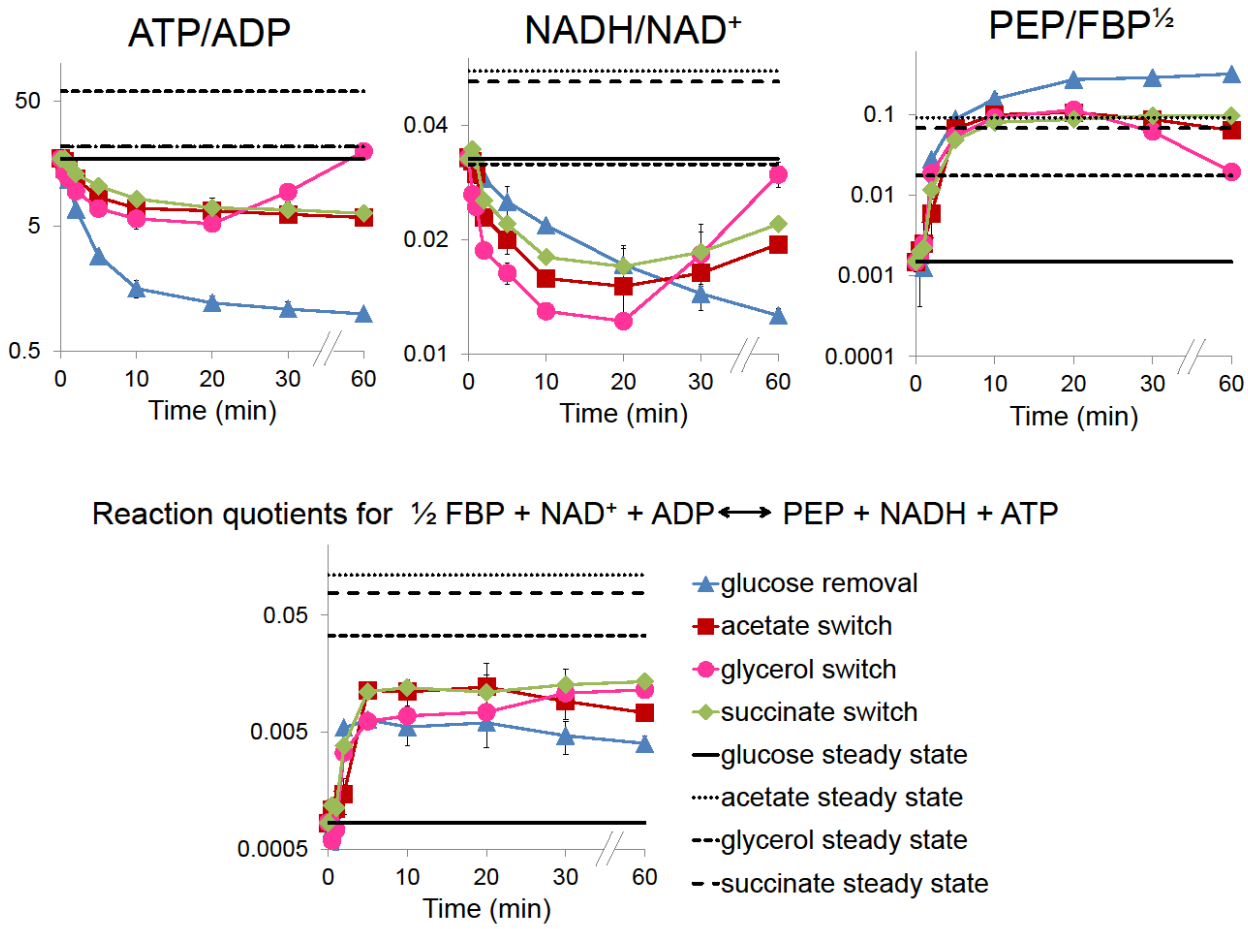

Supplementary Fig. 3. Upon glucose removal, decreasing ATP/ADP and NADH/NAD+ ratios drive carbon towards the bottom of glycolysis (i.e. towards PEP).

ATP/ADP and NADH/NAD$^+$ ratios decrease from 0 – 20 minutes after the switch in all four conditions, which overcomes the dramatic increase of PEP/FBP^{½} to drive carbon towards the bottom of glycolysis. Reaction quotients indicate the observed ratio of reactants to products. Lower quotient values favor downward reactions (i.e. towards PEP). The *x* axis represents minutes after the switch, and the *y* axis represents ratios and quotients in logarithmic scale. Points reflect data (mean ± range of N = 2 biological replicates).

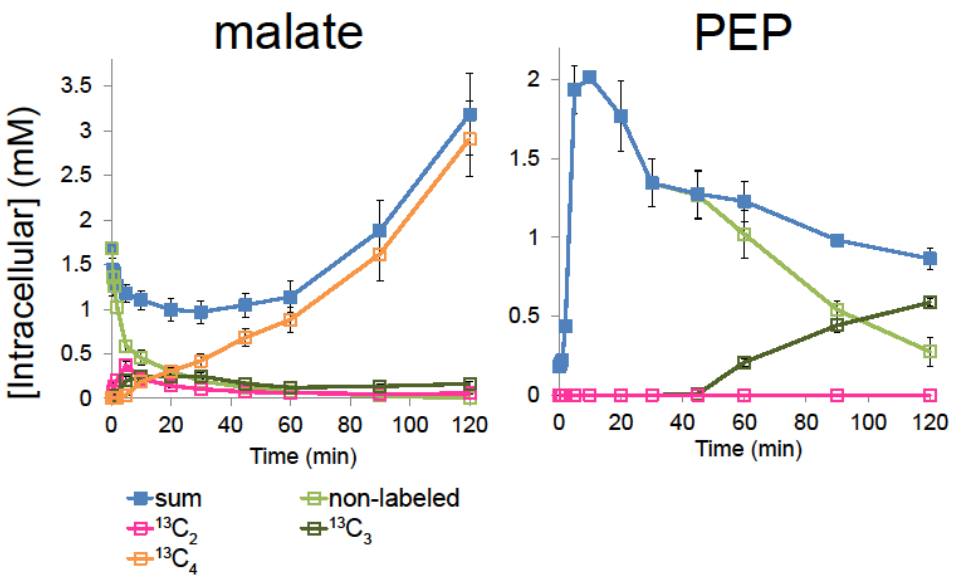

Supplementary Fig. 4. Accumulated PEP is not from gluconeogenesis or the PEP-glyoxylate cycle in the first 45 minutes after acetate switch.

E. coli wild type cells were switched from non-labeled glucose into U-^{13}C-acetate. While TCA compounds became labeled quickly, PEP did not get labeled until 1 h after the switch. $^{13}C_2$, $^{13}C_3$, and $^{13}C_4$ malate showed up in sequence due to the turning of TCA cycle. The *x* axis represents minutes after the switch, and the *y* axis represents absolute intracellular metabolite concentration. Points reflect data (mean ± range of N = 2 biological replicates).

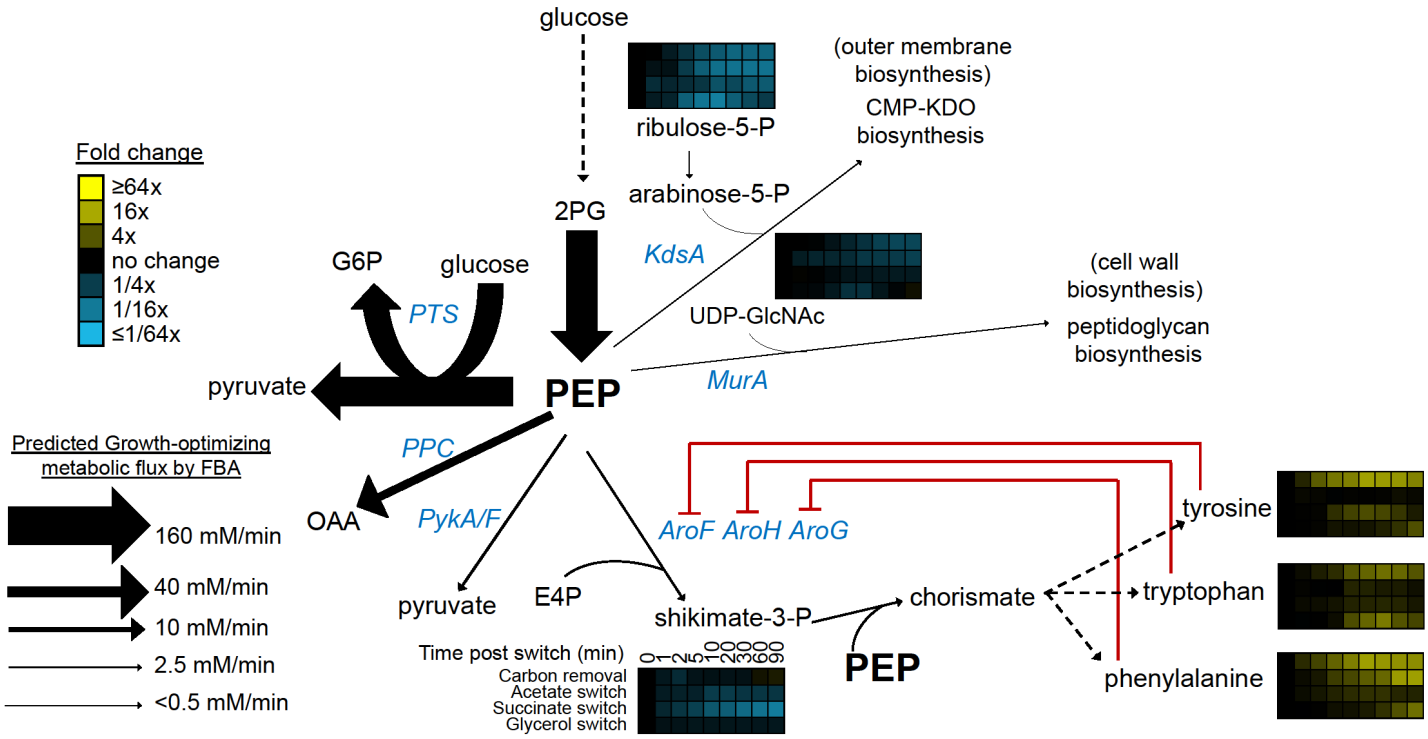

Supplementary Fig. 5. The primary PEP consuming enzymes are the PTS and PEP carboxylase.

All known PEP consumption routes are shown, along with concentration changes of associated metabolites upon glucose removal. Arrow sizes indicate steady state net fluxes from PEP for wild type *E. coli* cells growing freely on glucose filter cultures. The compound-specific heat maps match exactly the format of **Fig. 1**. E4P, erythrose-4-phosphate; shikimate-3-P, shikimate-3-phosphate; UDP-GlcNAc, UDP-*N*-acetyl-D-glucosamine; ribulose-5-P, ribulose-5-phosphate; arabinose-5-P, arabinose-5-phosphate; KDO, 2-Keto-3-Deoxy-D-*manno*-octonate.

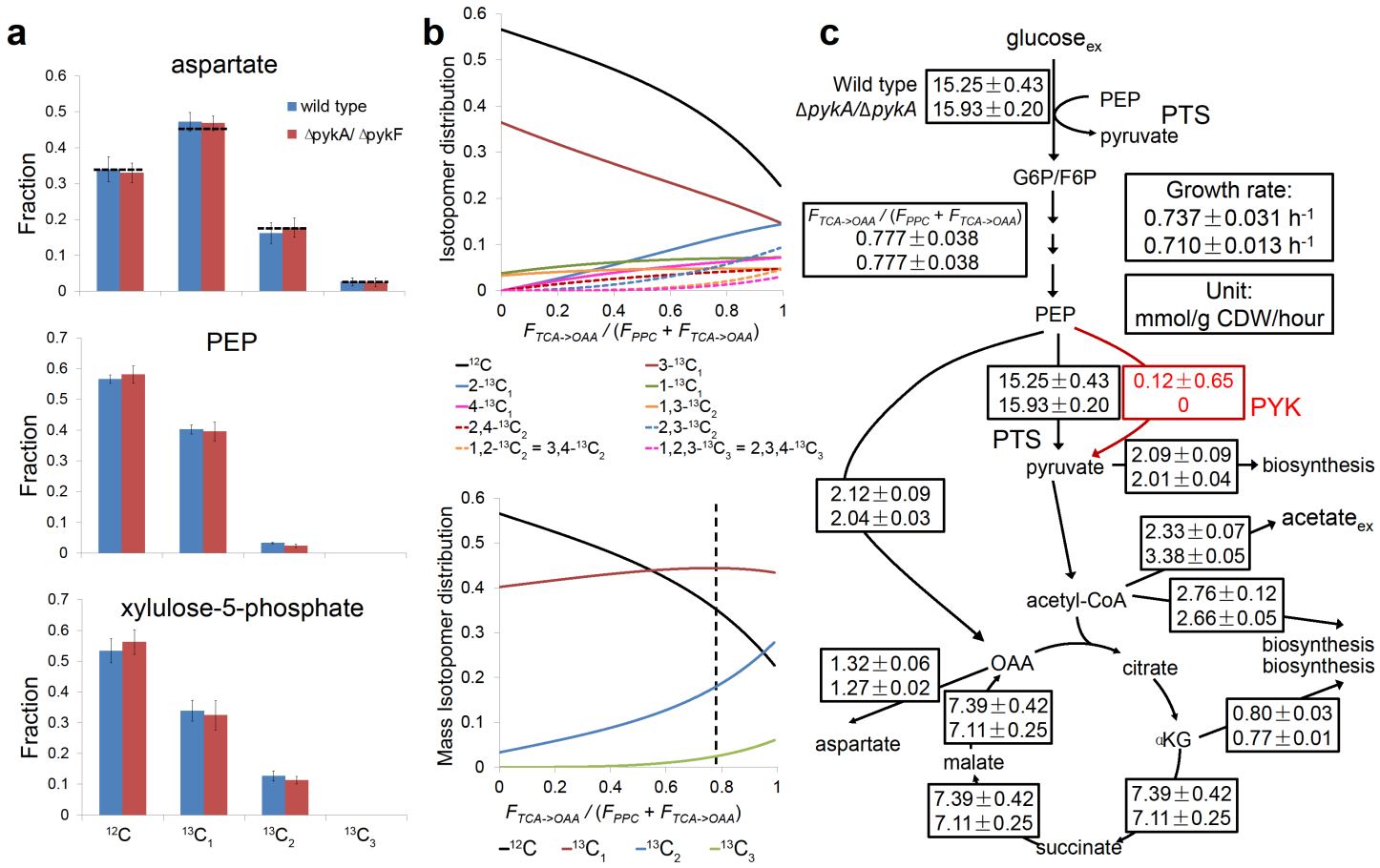

Supplementary Fig. 6. Metabolic Flux Analysis of wild type and Δ*pykA*/Δ*pykF* strains indicates pyruvate kinase flux accounts for < 5% of PEP consumption in wild type cells.

(**a**). Aspartate, PEP and xylulose-5-phosphate labeling patterns in wild type and Δ*pykA*/Δ*pykF* cells growing on 1-^{13}C glucose. Colored bars with error bars indicate mean ± SD of N = 6 biological replicates; dashed horizontal black lines in the aspartate panel indicate the theoretical labeling pattern given the calculated fluxes.

(**b**). Theoretical distribution of isopotomers (positionally labeled forms, upper panel) and mass isotopomers (sum of all positionally labeled forms with same number of labeled carbon atoms, lower panel) of aspartate as a function of TCA turning flux into oxaloacetate ($F_{TCA\rightarrow OAA}$) divided by sum of PEP carboxylase flux (F_{PPC}) and $F_{TCA\rightarrow OAA}$. The dashed vertical line indicates the experimentally observed value of $F_{TCA\rightarrow OAA}$ / (F_{PPC} + $F_{TCA\rightarrow OAA}$).

(**c**). Central carbon metabolic fluxes and error estimates in glucose-fed filter culture wild type and Δ*pykA*/Δ*pykF* cells. Reported values are best flux estimates +/- SE. For associated equations, see **Supplementary Methods**.

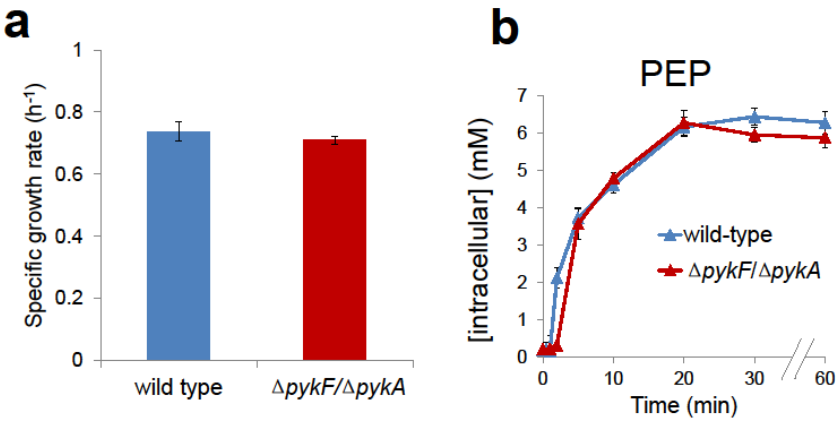

Supplementary Fig. 7. Deletion of pyruvate kinase (both isozymes, *pykA* and *pykF*) does not substantially alter *E. coli* growth or PEP concentration.

(**a**). Filter culture *E. coli* wild type and Δ*pykA*/Δ*pykF* cells were grown in glucose minimal media. Bars reflect data (mean ± range of N = 2 biological replicates).

(**b**). *E. coli* wild type and Δ*pykA*/Δ*pykF* cells were switched from glucose to no carbon. The *x* axis represents minutes after the switch, and the *y* axis represents absolute intracellular PEP concentration. Points reflect data (mean ± range of N = 2 biological replicates).

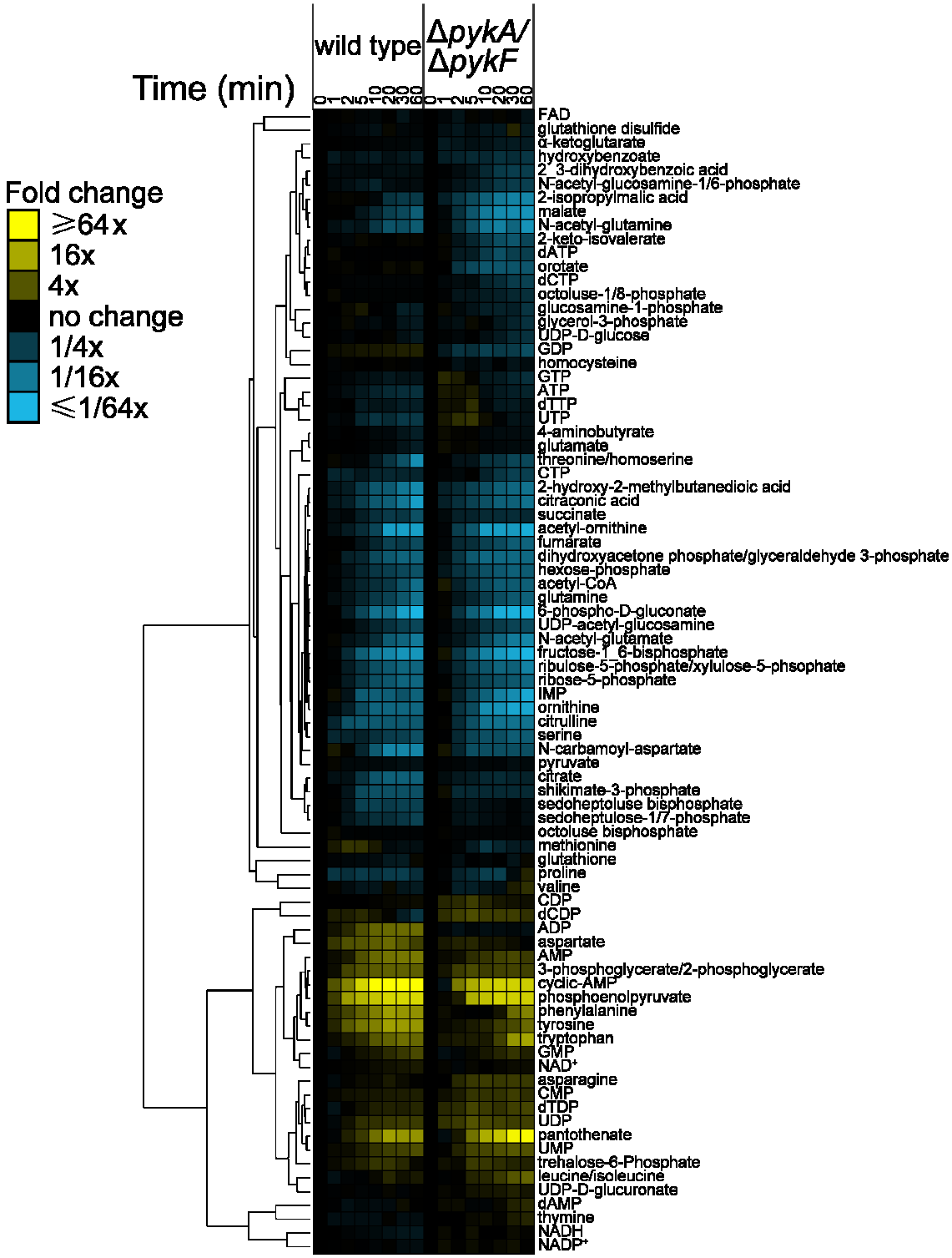

Supplementary Fig. 8. Impact of pyruvate kinase deletion (both isozymes, *pykA* and *pykF*) on *E. coli* metabolome response to glucose removal. Metabolite levels of biological duplicates were averaged, normalized to cells growing steadily in glucose (time zero), and the resulting fold changes log transformed and shown in heat map format.

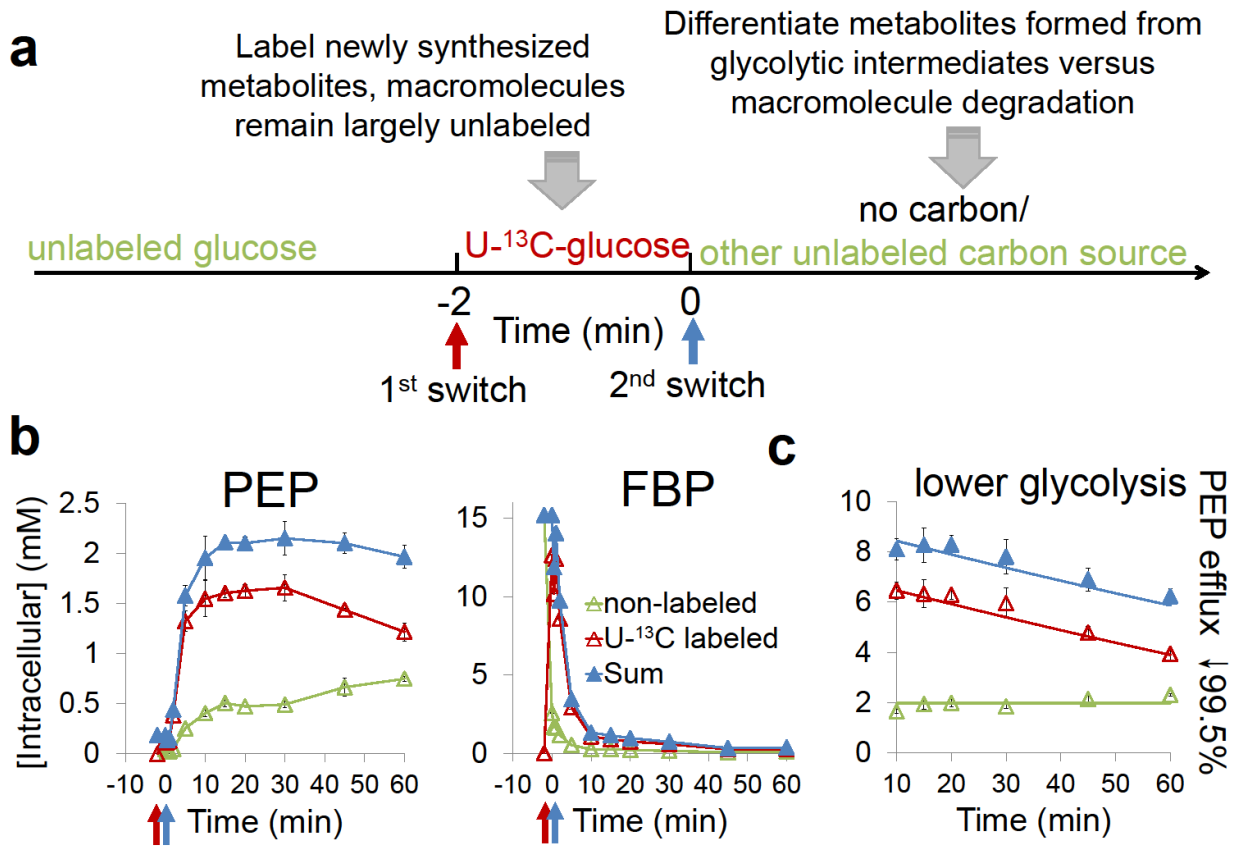

Supplementary Fig. 9. Transient labeling experiment as per Fig. 2 of main text, except with shorter labeling duration.

Methods are the same as **Fig. 2a** and **c** of main text except with 2 min labeling duration. Data were data analyzed using main text **Equations (3)** and **(4)** to give decrease in PEP efflux of 99.5%, versus 99.6% in **Fig. 2c**.

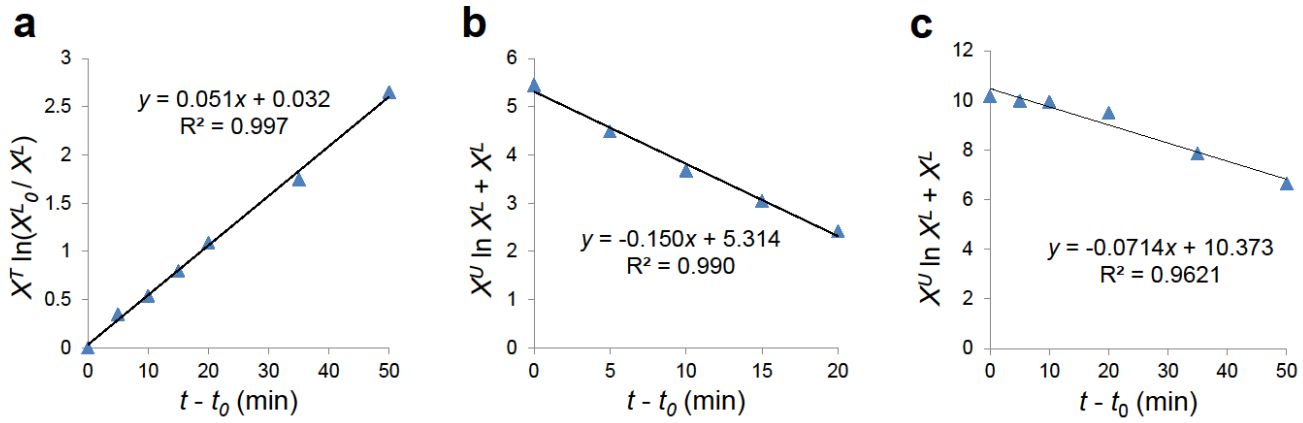

Supplementary Fig. 10. Fit of experimental data to equations used for quantitation of PEP consumption during carbon starvation and acetate switch based on transient labeling experiments with (a) 8 min ^{13}C-glucose labeling followed by carbon starvation, (b) 8 min ^{13}C-glucose labeling followed by acetate switch, and (c) 2 min ^{13}C-glucose labeling followed by carbon starvation.

(**a**). The plot ($X^T \ln(X^L_0/X^L)$) vs. ($t - t_0$) gives a straight line, consistent with a steady unlabeled production flux and a matching steady consumption flux from PEP (for details see **Methods**). The slope gives f = 0.051 mM/min, which is 99.6% less than PEP carboxylase flux in the glucose-fed cells.

(**b**). The plot ($X^U \ln X^L + X^L$) vs. ($t - t_0$) gives a straight line, indicating a decreasing unlabeled production flux and a steady consumption flux from PEP. The slope gives f_{ex} = 0.15 mM/min, which requires a 99.0% inhibition of PEP carboxylase.

(**c**). The plot ($X^U \ln X^L + X^L$) vs. ($t - t_0$) gives a straight line, consistent with a decreasing unlabeled production flux and a steady consumption flux from PEP. The slope gives f_{ex} = 0.071 mM/min, which is 99.5% less than PEP carboxylase flux in the glucose-fed cells.

Points reflect data; lines represent least square fitting.

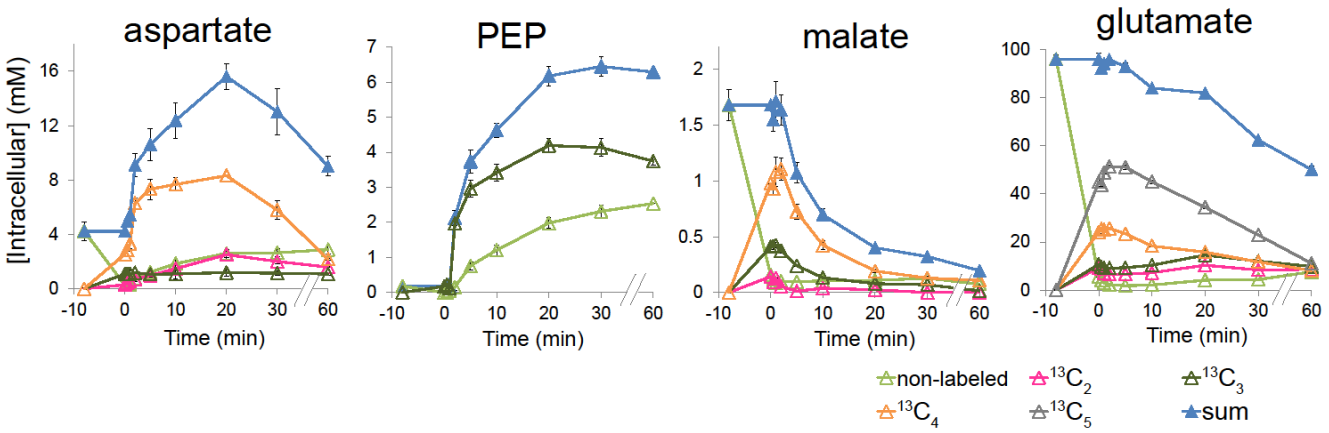

Supplementary Fig. 11. Accumulated aspartate is not from anapleurosis.

Glycolytic intermediates were labeled by switching cells to U-^{13}C-glucose for 8 min. Thereafter, glucose was removed and replaced with no carbon. The majority of accumulated aspartate is fully ($^{13}C_4$) labeled. As fully labeled glutamate declines in parallel with the rise in aspartate, the increase in aspartate is likely fed by turning of the TCA cycle, combined with decreased aspartate consumption to protein and pyrimidine synthesis. Anapleurosis from PEP would result in triply-labeled ($^{13}C_3$) aspartate, containing one unlabeled carbon atom from bicarbonate. Such aspartate does not accumulate, consistent with the evidence that anapleurosis terminates almost completely. The *x* axis represents minutes after carbon starvation, and the *y* axis represents absolute intracellular concentration. Points reflect data (mean ± range of N = 2 biological replicates).

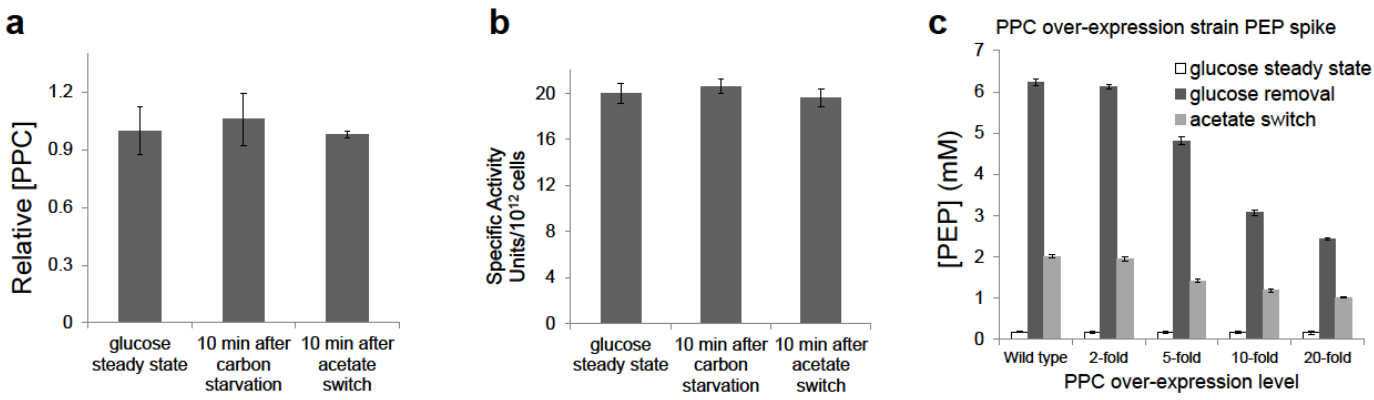

Supplementary Fig. 12. There is no degradation or stable, inactivating post-translational modification of PEP carboxylase in the first 10 minutes following glucose removal.

(**a**). PEP carboxylase protein concentration is the same before and after glucose removal. Wild type *E. coli* cells growing freely in glucose minimal media were switched to no carbon or acetate as indicated. After 10 minutes of glucose removal, PEP carboxylase (PPC) protein concentration was quantitated by targeted LC-MS (see **Methods**). The *y* axis represents relative PEP carboxylase protein concentration (glucose-fed wild type cells defined as 1). Bars reflect data (mean ± range of N = 2 biological replicates). (**b**). PEP carboxylase activity is the same in the cell lysates before and after the switches, indicating no stable, inactivating post-translational modification of PEP carboxylase during glucose removal[25]. PEP carboxylase activity was measured in the presence of PEP (0.18 mM) and the essential activator acetyl-CoA (0.61 mM).The *y* axis represents specific enzyme activity in Units (µmol of product produced per minute) per 10^{12} cells. Bars reflect data (mean ± range of N = 2 biological replicates). (**c**). While over-expression of PEP carboxylase modestly reduces the basal PEP concentration in glucose-fed cells, it does not block the PEP spike after glucose removal. Carbon starvation and acetate switch were performed on WT/pCA24N-*ppc* strain with different induction levels of PEP carboxylase. The *x* axis reports these levels as fold-increase versus wild type cells as quantitated by targeted LC-MS. IPTG levels were 20, 50, 100 and 200 µM for the 2-, 5-, 10- and 20-fold over-expression levels, respectively. The *y* axis represents absolute intracellular PEP concentration. Bars reflect data (mean ± range of N = 2 biological replicates).

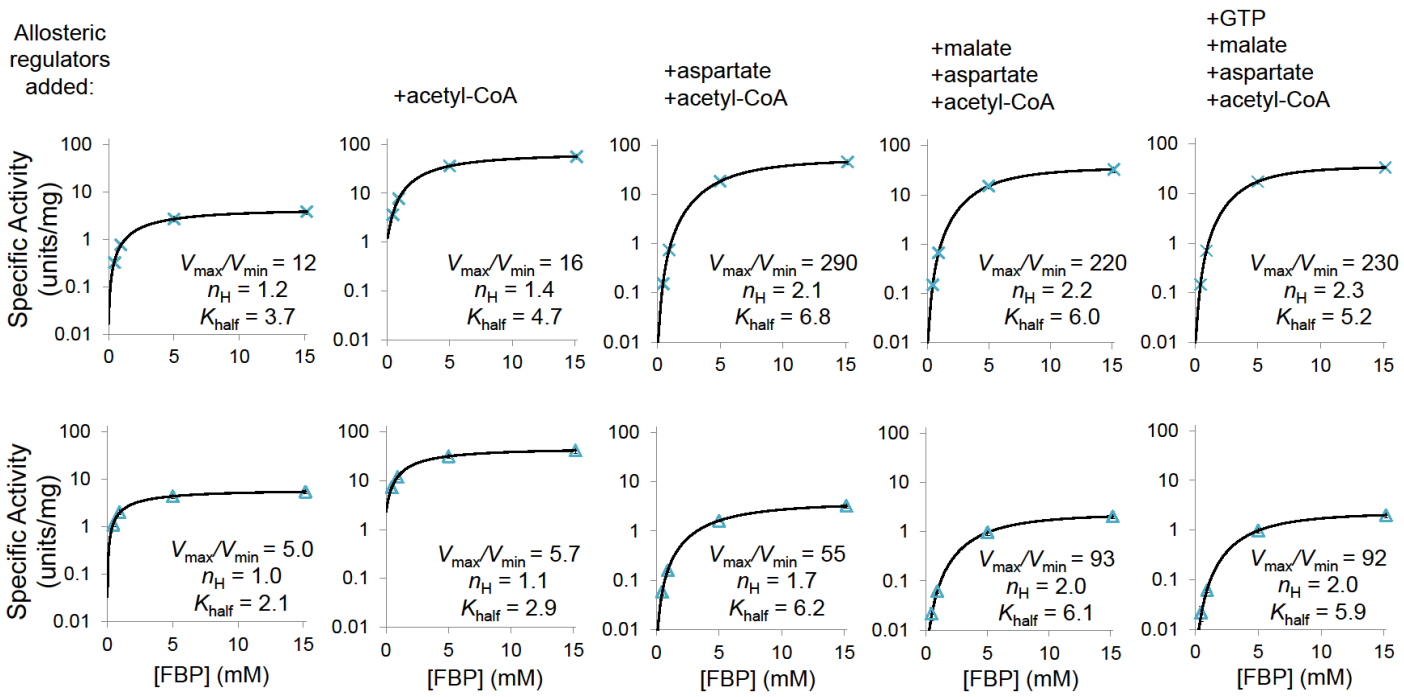

Supplementary Fig. 13. The enhancement of FBP activation by acetyl-CoA and aspartate was also found when effectors were added at their physiological concentrations in glucose minimal media and carbon starvation conditions.

Each small plot shows activity of purified His-tagged PEP carboxylase as a function of FBP concentration. The concentration of PEP and effectors were selected to match the physiological concentration in cells growing in steady state on glucose minimal media (top row, cross markers) and switched to no carbon for 10 min (bottom row, triangle markers). Top row concentrations are: PEP, 0.18 mM; acetyl-CoA, 0.61 mM; aspartate, 4.2 mM; malate, 1.7 mM; GTP, 4.9 mM. Bottom row concentrations are: PEP, 4.7 mM; acetyl-CoA, 0.21 mM; aspartate, 19 mM; malate, 0.7 mM, GTP, 2.1 mM. Bicarbonate and cofactor magnesium was added both at 10 mM. The *x* axis represents different FBP concentrations, and the logarithmic *y* axis represents specific PEP carboxylase activity in enzyme activity Units (µmol of product produced per minute) per mg of enzyme. Experimental data (mean ± range of N = 2) were fitted to Hill-equations (lines). V_{max}/V_{min} represents observed range of PEP carboxylase activity as a function of FBP concentration, where V_{max} was measured at 15 mM FBP, matching the physiological concentration in cells growing on glucose, and V_{min} was measured at 0,45 mM FBP, matching the physiological FBP concentration in cells switched from glucose to acetate for 10 minutes. n_H and K_{half} represent the Hill-coefficient for FBP and the FBP concentration producing half-maximal activation.

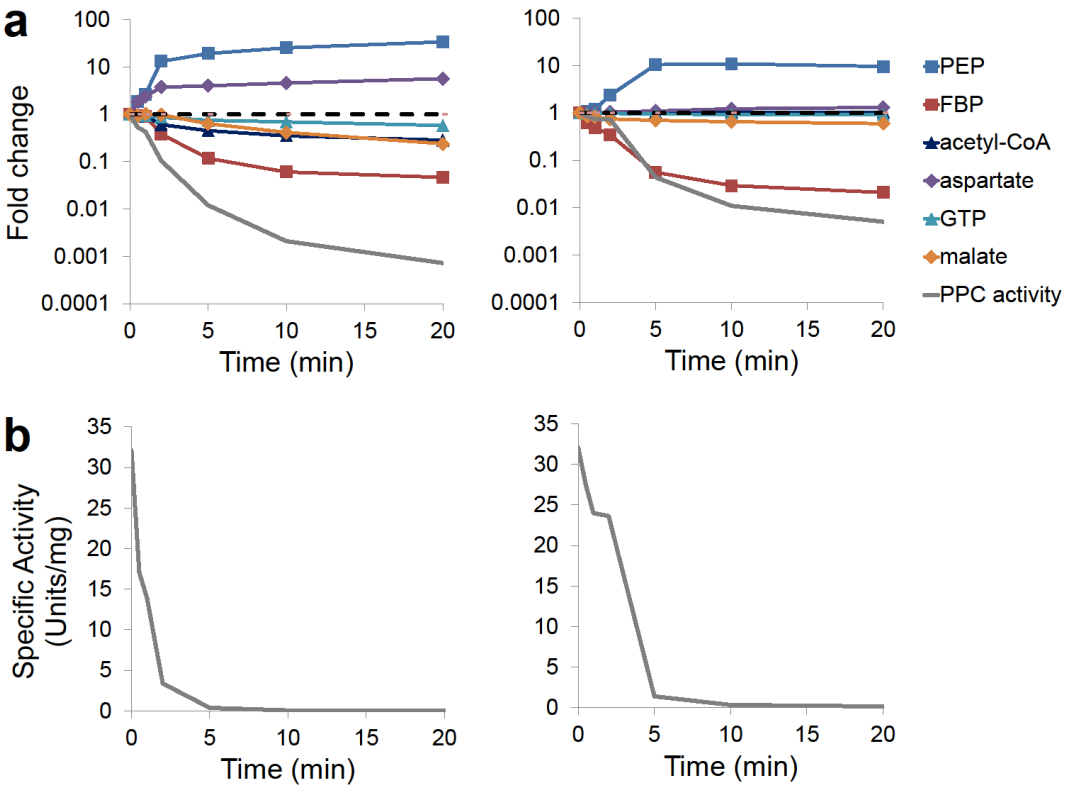

Supplementary Fig. 14. Inferred PEP carboxylase activity in live cells following glucose removal.

(**a**). Fold change (in logarithmic scale) of PEP and PEP carboxylase's allosteric regulator's concentrations over the first 20 minutes after carbon starvation (left) and acetate switch (right), and associated inferred PEP carboxylase activity.

(**b**). Inferred PEP carboxylase specific activity over the first 20 minutes after carbon starvation (left) and acetate switch (right) on linear axis.

PEP carboxylase activity was calculated from the biochemistry data shown in **Fig. 3**, **Supplementary Fig. 13** and **17**. Data points are experimental measurements. Lines connect measured (or, in the case of PEP carboxylase activity, calculated) values at the time points where measurementswere taken.

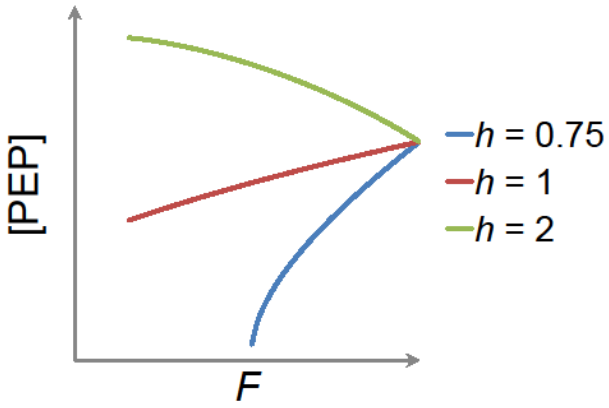

Supplementary Fig. 15. Ultrasensitive regulation of PEP carboxylase is required for PEP to increase when glycolytic influx decreases.

The simplified glycolytic model shown in **Scheme 1** was solved quantitatively for [PEP] as a function of glycolytic flux *F*. The hill coefficient for activation of PEP carboxylase (*h*) determines the qualitative pattern of the PEP response, with $h > 1$ required for PEP to increase when F decreases. Both the *x* and *y* axis are presented in arbitrary units; the units depend on other parameters of the model, but the trends are identical irrespective of these parameters.

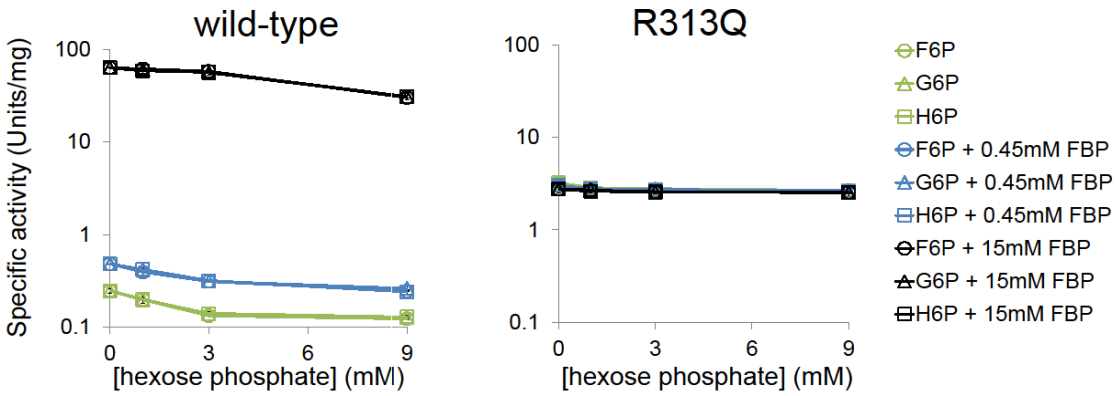

Supplementary Fig. 16. PEP carboxylase is not activated by glucose-6-phosphate or fructose-6-phosphate.

Each plot shows activity of purified His-tagged PEP carboxylase as a function of the concentration of the indicated phosphorylated hexose sugar. The concentration of PEP (2 mM), as well as effectors acetyl-CoA (0.63 mM), aspartate (5.2 mM), malate (1.1 mM), and GTP (4.6 mM) were selected to match the physiological concentration in cells switched from glucose to acetate for 10 minutes. FBP was either not added, or added at 0.45 mM (to match the physiological concentration in cells switched from glucose to acetate for 10 minutes), or 15 mM (to match the physiological concentration in cells growing in steady state on glucose minimal media). The *x* axis represents the concentration of the indicated phosphorylated hexose sugar: F6P (fructose-6-phosphate alone, round markers), G6P (glucose-6-phosphate along, triangle markers), or H6P (50:50 mix of fructose-6-phosphate : glucose-6-phosphate, square markers). The logarithmic *y* axis represents specific PEP carboxylase activity in enzyme activity Units (µmol of product produced per minute) per mg of enzyme. Points reflect data (mean ± range of N = 2 biological replicates).

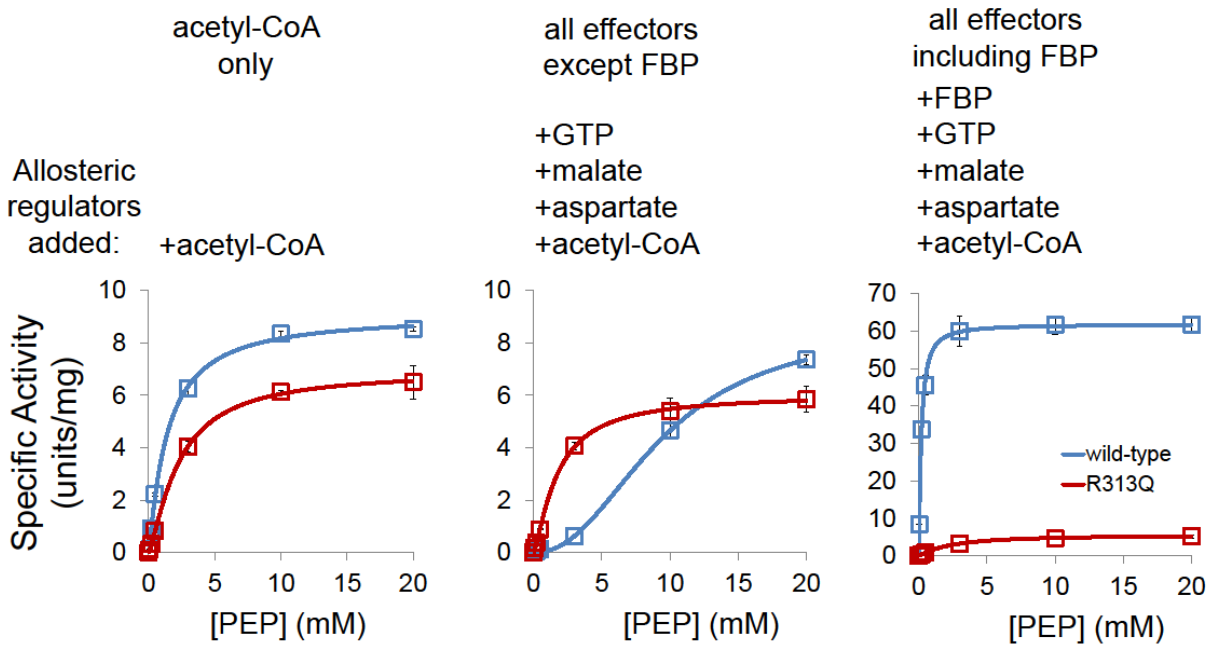

Supplementary Fig. 17. Determination of PEP carboxylase wild type and R313Q kinetic parameters.

Each plot shows the activity of purified His-tagged PEP carboxylase as a function of PEP concentration. The concentrations of the effectors acetyl-CoA (0.63 mM), FBP (15 mM), aspartate (5.2 mM), malate (1.1 mM), and GTP (4.6 mM) were selected to match the physiological concentration in cells switched from glucose to acetate for 10 minutes. See **Supplementary Table 2** for kinetic parameters. The *x* axis represents different PEP concentrations, and the *y* axis represents specific PEP carboxylase activity in enzyme activity Units (µmol of product produced per minute) per mg of enzyme. Experimental data (mean ± range of N = 2) were fitted to Hill-equations (lines).

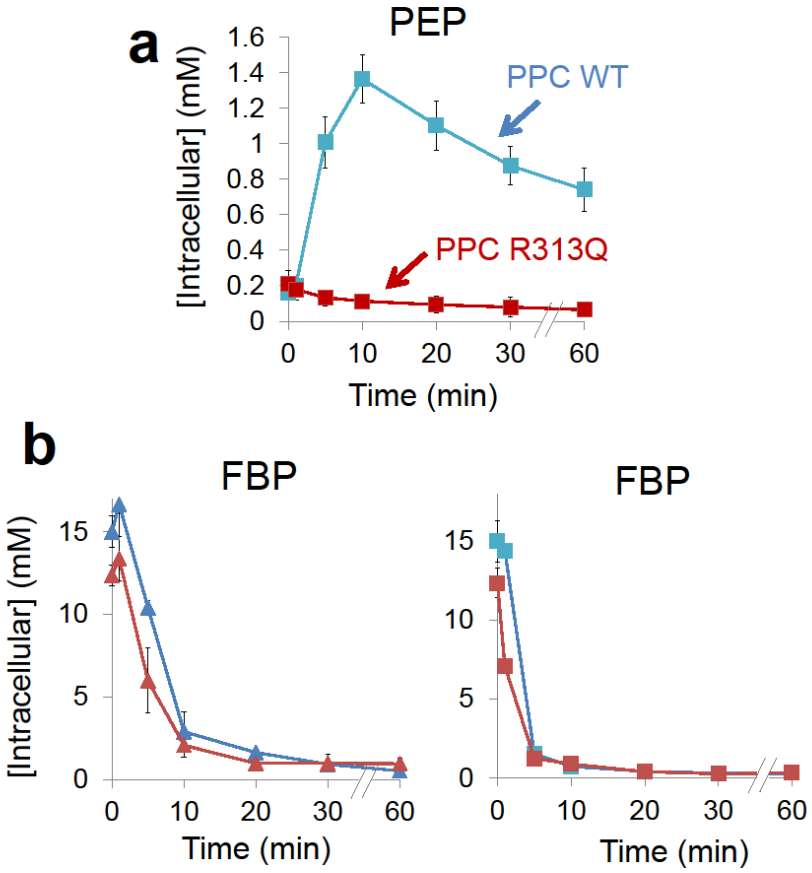

Supplementary Fig. 18. Expression of PEP carboxylase R313Q ablates the PEP spike while FBP decreases as normal.

(**a**). *E. coli* strains in which endogenous PEP carboxylase has been replaced with inducible expression of wild type enzyme (Δ*ppc*/pCA24N-*ppc*) or the FBP-insensitive R313Q mutant (Δ*ppc*/pCA24N-*ppc*R313Q) were switched to acetate.

(**b**). The above strains were switched to either no carbon (left) or acetate (right).

The *x* axis represents minutes after the switch, and the *y* axis represents absolute intracellular metabolite concentration. Points reflect data (mean ± range of N = 2 biological replicates).

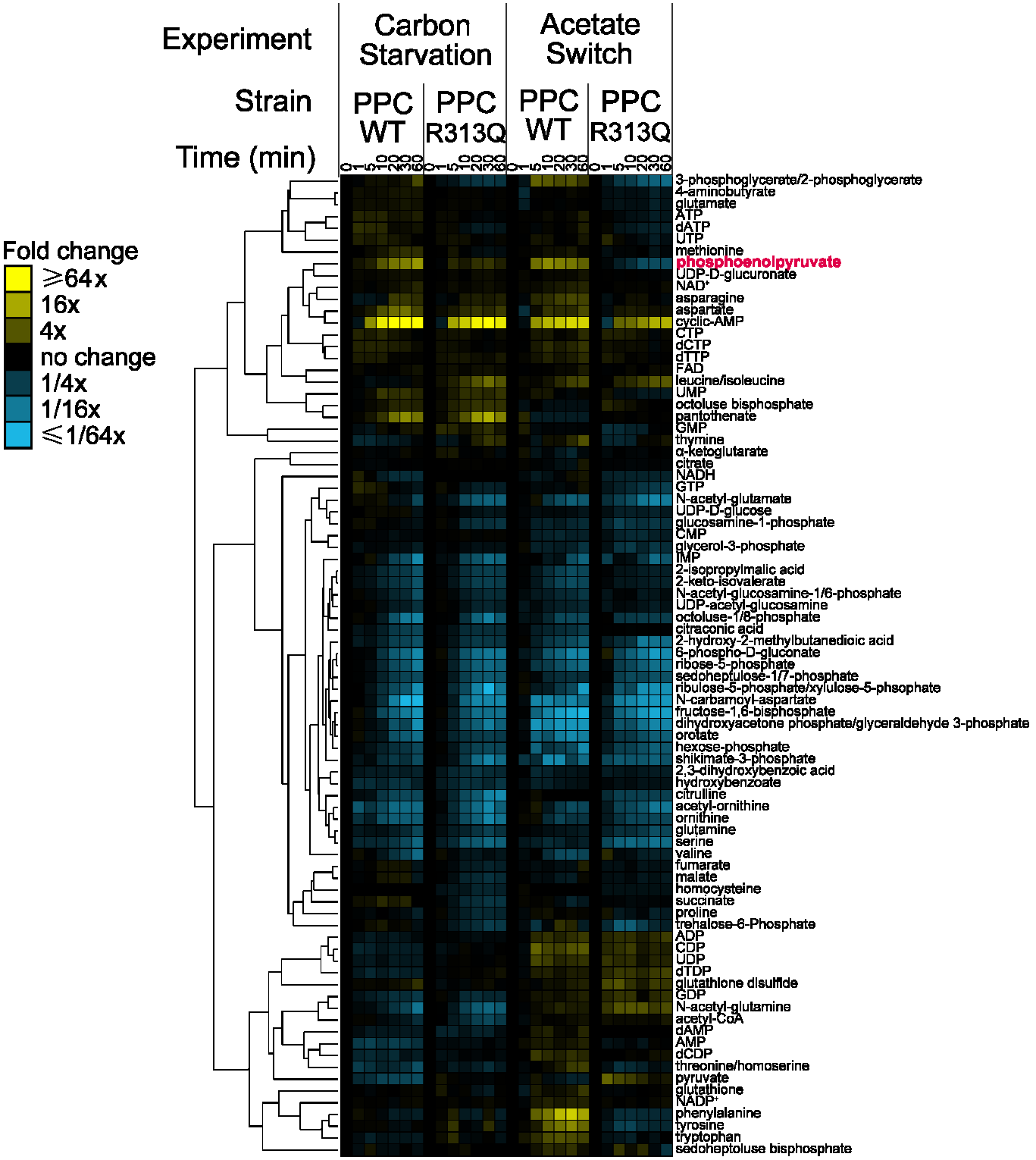

Supplementary Fig. 19. Heat map of all measured metabolites in the Δ*ppc*/pCA24N-*ppc* (PPC WT) and Δ*ppc*/pCA24N-*ppc*R313Q (PPC R313Q) during glucose removal and its replacement with no carbon or acetate.

Metabolite levels of biological duplicates were averaged, normalized to cells growing steadily in glucose (time zero), and the resulting fold changes log transformed.

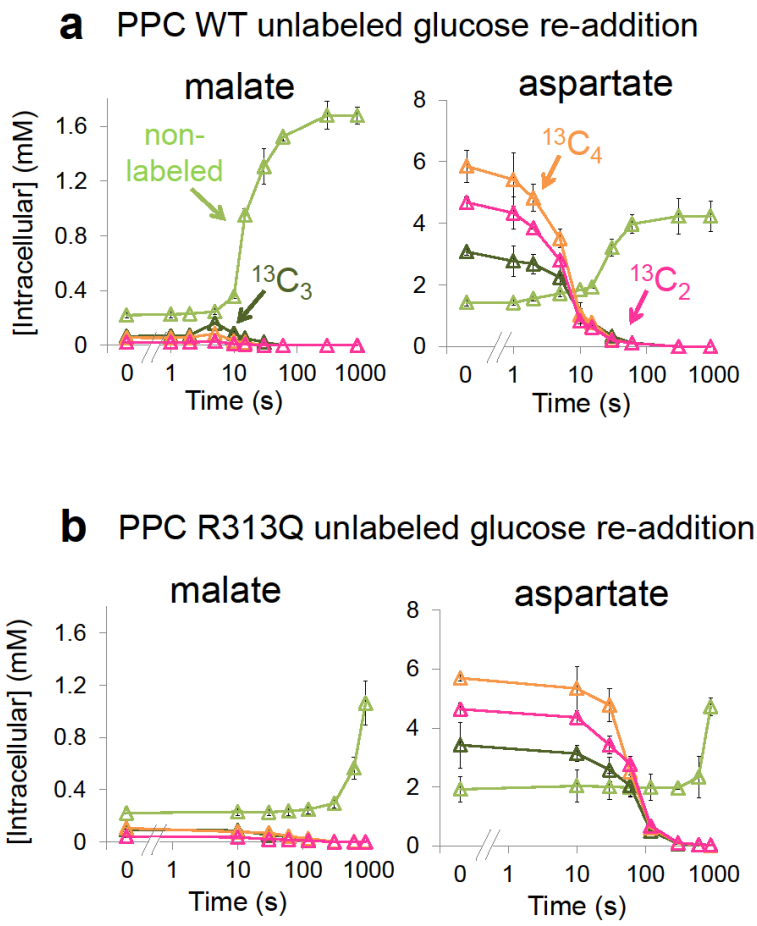

Supplementary Fig. 20. The reserve of PEP is required for rapid initiation of anapleurosis upon glucose re-addition.

Δ*ppc*/pCA24N-*ppc* (PPC WT) and Δ*ppc*/pCA24N-*ppc*R313Q (PPC R313Q) were switched to U-^{13}C-glucose for 8 minutes, followed by no carbon for 30 minutes, and finally re-addition of unlabeled glucose. Upon glucose re-addition, samples were collected and intracellular metabolites (labeled and unlabeled) quantitated by LC-MS. Experiments were performed in the presence of 100 µM IPTG.

(a) For Δ*ppc*/pCA24N-*ppc*, malate starts to increase quickly after glucose readdition and reaches normal steady state levels within 1 minute. This increase of malate is not from aspartate: While all the ^{13}C forms of aspartate decrease after the glucose re-addition, only three-^{13}C malate shows a spike, indicating its glycolytic origin.

(b) For Δ*ppc*/pCA24N-*ppc*R313Q, due to the failure to accumulate PEP during glucose starvation and consequent slow increase of FBP upon glucose re-addition, malate did not increase until 7 minutes after glucose re-addition.

The *x* axis represents seconds after glucose re-addition (in logarithmic scale), and the *y* axis represents absolute intracellular concentration. Points reflect data (mean ± range of N = 2 biological replicates).

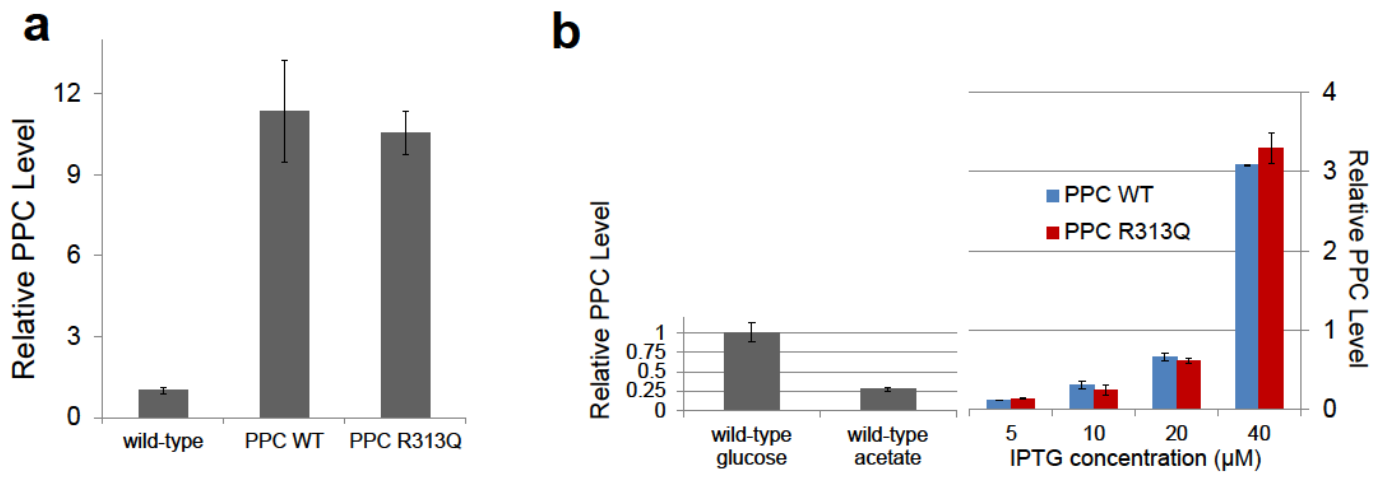

Supplementary Fig. 21. Quantitation of PEP carboxylase protein concentration in cells growing on glucose or acetate, with or without inducible expression from plasmid with IPTG.

(**a**). Identical inducible expression wild type and R313Q PEP carboxylase. Wild type *E. coli*, Δ*ppc*/pCA24N-*ppc* (PPC WT), and Δ*ppc*/pCA24N-*ppc*R313Q (PPC R313Q) cells were grown in glucose minimal media, with the latter two strains grown in the presence of 100 μM IPTG.

(**b**). Left panel: PEP carboxylase protein concentration in wild type *E. coli* cells growing on acetate is ~25% compared to protein concentration of wild type cells growing on glucose. Right panel: In the presence of 10 μM IPTG, PEP carboxylase protein concentration in PPC WT and PPC R313Q were approximately equal to protein concentration of wild type cells growing on acetate. Wild type *E. coli*, PPC WT, and PPC R313Q were grown in either glucose or acetate minimal media, with the latter two strains in the presence of indicated concentration of IPTG.

In both (a) and (b), PEP carboxylase protein concentration was quantitated by SDS-PAGE followed by targeted LC-MS/MS. The *y* axis represents the relative enzyme level (PEP carboxylase concentration in wild type *E. coli* cells growing on glucose defined as 1). Bars reflect data (mean ± range of N = 2 biological replicates).

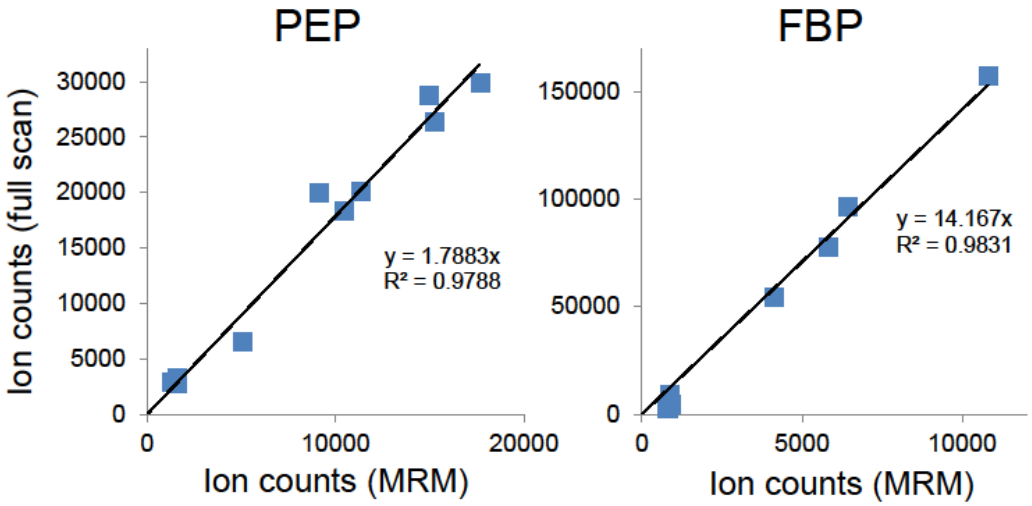

Supplementary Fig. 22. LC-high resolution MS analysis and LC-triple quadrupole MS/MS analysis yield similar data.

Exemplary data are shown for the switch from glucose to acetate. The plots show raw ion counts for the indicated compound from the targeted LC-triple quadrupole MS/MS analysis (multiple reaction monitoring, or MRM) (x-axis) and from the LC-high resolution MS analysis (full scan) (y-axis). The results are linearly correlated with $R^2 > 0.97$. Points reflect means of two independent measurements by each method; lines represent least square fitting.

Supplementary Table 1. Intracellular concentrations of PEP, FBP, acetyl-CoA, aspartate, malate, and GTP in *E. coli* during different growth conditions as measured by LC-MS.

Condition	PEP (mM)	FBP (mM)	acetyl-CoA (mM)	aspartate (mM)	malate (mM)	GTP (mM)
glucose minimal media	0.18	15	0.61	4.2	1.7	4.9
switch to acetate for 10 min	2.0	0.45	0.63	5.2	1.1	4.6
removal of carbon for 10 min	4.7	0.92	0.21	19	0.70	2.1

Supplementary Table 2. Kinetic parameters of purified wild type and R313Q PEP carboxylase. The effector concentrations of acetyl-CoA (0.63 mM), FBP (15 mM), aspartate (5.2 mM), malate (1.1 mM), and GTP (4.6 mM) were selected to match the physiological concentration in cells switched from glucose to acetate for 10 minutes. PEP was added in a range of 0-20 mM. K_m represents PEP concentration at which reaction rate is half-maximum. Three conditions were investigated: acetyl-CoA only, all effectors except FBP, and all effectors including FBP. Data without any effectors is not reported, as the enzyme activity is minimal in the absence of acetyl-CoA.

	K_m (mM) for PEP		**Turnover number (min^{-1})**		**Hill-coefficient for PEP**	
condition	Wild type	R313Q	Wild type	R313Q	Wild type	R313Q
acetyl-CoA only	1.4	2.3	910	690	1.1	1.3
all effectors except FBP	9.4	1.8	870	600	2.2	1.3
all effectors including FBP	0.2	2.3	6200	560	1.2	1.2

Supplementary Table 3. Mass, retention time, and signal intensity of measured metabolites by the LC-high resolution MS analysis.

	formula	m/z	retention time (min)	average intensity in samples from glucose-fed cells
Pyruvate	$C_3H_4O_3$	87.0088	8.3	38200
4-aminobutyrate	$C_4H_9NO_2$	102.0561	4.5	353411
Serine	$C_3H_7NO_3$	104.0353	1	112723
Proline	$C_5H_9NO_2$	114.0561	1.12	15072
Fumarate	$C_4H_4O_4$	115.0037	13.4	34524
2-keto-isovalerate	$C_5H_8O_3$	115.0401	13.06	33289
Valine	$C_5H_{11}NO_2$	116.0717	1	43363
Succinate	$C_4H_6O_4$	117.0193	11.6	49220
threonine/homoserine	$C_4H_9NO_3$	118.051	1	182229
Thymine	$C_5H_6N_2O_2$	125.0357	2.6	5783
citraconic acid	$C_5H_6O_4$	129.0193	12.95	216516
leucine/isoleucine	$C_6H_{13}NO_2$	130.0874	1.9	79015
asparagines	$C_4H_8N_2O_3$	131.0462	1	7816
Ornithine	$C_5H_{12}N_2O_2$	131.0826	1	15785
Aspartate	$C_4H_7NO_4$	132.0302	4.4	30804
Malate	$C_4H_6O_5$	133.0143	12.7	64026
Homocysteine	$C_4H_9NO_2S$	134.0281	1	1716
Hydroxybenzoate	$C_7H_6O_3$	137.0244	10.88	7387
α-ketoglutarate	$C_5H_6O_5$	145.0143	13.1	6383
Glutamine	$C_5H_{10}N_2O_3$	145.0619	1	278323
Glutamate	$C_5H_9NO_4$	146.0459	4.6	836814
2-hydroxy-2-methylbutanedioic acid	$C_5H_8O_5$	147.0299	12.6	178898
methionine	$C_5H_{11}NO_2S$	148.0438	1.6	12705
2,3-dihydroxybenzoic acid	$C_7H_6O_4$	153.0193	13.58	12010
orotate	$C_5H_4N_2O_4$	155.0098	8.1	65364
phenylalanine	$C_9H_{11}NO_2$	164.0717	4.1	8084
phosphoenolpyruvate	$C_3H_5O_6P$	166.9751	13.7	1750
DHAP/GAP	$C_3H_7O_6P$	168.9908	9.3	45599
glycerol-3-phosphate	$C_3H_9O_6P$	171.0064	7.3	109925
acetyl-ornithine	$C_7H_{14}N_2O_3$	173.0932	1	29588
citrulline	$C_6H_{13}N_3O_3$	174.0884	0.9	5549
N-carbamoyl-aspartate	$C_5H_8N_2O_5$	175.036	12	43638
2-isopropylmalic acid	$C_7H_{12}O_5$	175.0612	13.94	212239
tyrosine	$C_9H_{11}NO_3$	180.0666	2	15763
3-phosphoglycerate/2-phosphoglycerate	$C_3H_7O_7P$	184.9857	13.58	46101

	formula	m/z	retention time (min)	average intensity in samples from glucose-fed cells
N-acetyl-glutamine	$C_7H_{12}N_2O_4$	187.0724	7	54300
N-acetyl-glutamate	$C_7H_{11}NO_5$	188.0564	13	228460
citrate	$C_6H_8O_7$	191.0197	13.6	305171
tryptophan	$C_{11}H_{12}N_2O_2$	203.0826	7.6	1897
pantothenate	$C_9H_{17}NO_5$	218.1034	11	7309
ribose-5-phosphate	$C_5H_{11}O_8P$	229.0119	7.2	73902
ribulose-5-phosphate/xylulose-5-phsophate	$C_5H_{11}O_8P$	229.0119	7.8	37402
shikimate-3-phosphate	$C_7H_{11}O_8P$	253.0119	13.44	8185
glucosamine-1-phosphate	$C_6H_{14}NO_8P$	258.0384	1.5	6610
hexose-phosphate	$C_6H_{13}O_9P$	259.0224	6.9	2092317
6-phospho-D-gluconate	$C_6H_{13}O_{10}P$	275.0174	13.38	135995
sedoheptulose-1/7-phosphate	$C_7H_{15}O_{10}P$	289.033	6.95	127886
N-acetyl-glucosamine-1/6-phosphate	$C_8H_{16}NO_9P$	300.049	7.3	41778
glutathione	$C_{10}H_{17}N_3O_6S$	306.0765	8	1839115
octoluse bisphosphate	$C_8H_{17}O_{11}P$	319.0436	13.64	8372
CMP	$C_9H_{14}N_3O_8P$	322.0446	8.7	6010
UMP	$C_9H_{13}N_2O_9P$	323.0286	10.2	6346
cyclic-AMP	$C_{10}H_{12}N_5O_6P$	328.0453	12.6	4107
dAMP	$C_{10}H_{14}N_5O_6P$	330.0609	12	9898
fructose-1,6-bisphosphate	$C_6H_{14}O_{12}P_2$	338.9888	13.5	381898
trehalose/sucrose	$C_{12}H_{22}O_{11}$	341.109	1.18	27378
AMP	$C_{10}H_{14}N_5O_7P$	346.0558	11.3	34866
IMP	$C_{10}H_{13}N_4O_8P$	347.0398	10.7	18055
GMP	$C_{10}H_{14}N_5O_8P$	362.0507	10.7	6796
sedoheptoluse bisphosphate	$C_7H_{15}O_{10}P$	368.9993	13.64	36022
dCDP	$C_9H_{15}N_3O_{10}P_2$	386.016	13.58	7768
octoluse 8/1P	$C_8H_{18}O_{14}P_2$	399.0099	6	10120
dTDP	$C_{10}H_{16}N_2O_{11}P_2$	401.0157	13.58	36699
CDP	$C_9H_{15}N_3O_{11}P_2$	402.0109	13.3	3944
UDP	$C_9H_{14}N_2O_{12}P_2$	402.9949	13.5	20545
trehalose-6-Phosphate	$C_{12}H_{23}O_{14}P$	421.0753	7.2	9221
ADP	$C_{10}H_{15}N_5O_{10}P_2$	426.0221	13.7	158485
GDP	$C_{10}H_{15}N_5O_{11}P_2$	442.0171	13.5	28468
dCTP	$C_9H_{16}N_3O_{13}P_3$	465.9823	14.8	25053
dTTP	$C_{10}H_{17}N_2O_{14}P_3$	480.982	14.94	196251
CTP	$C_9H_{16}N_3O_{14}P_3$	481.9772	14.8	151378
UTP	$C_9H_{15}N_2O_{15}P_3$	482.9612	15	446726
dATP	$C_{10}H_{16}N_5O_{12}P_3$	489.9936	14.94	41853
ATP	$C_{10}H_{16}N_5O_{13}P_3$	505.9885	15.1	1621122
GTP	$C_{10}H_{16}N_5O_{14}P_3$	521.9834	15	217619

	formula	m/z	retention time (min)	average intensity in samples from glucose-fed cells
UDP-D-glucose	$C_{15}H_{24}N_2O_{17}P_2$	565.0477	13.25	1483574
UDP-D-glucuronate	$C_{15}H_{22}N_2O_{18}P_2$	579.027	14.7	766639
UDP-acetyl-glucosamine	$C_{17}H_{27}N_3O_{17}P_2$	606.0743	13.27	1009912
glutathione disulfide	$C_{20}H_{32}N_6O_{12}S_2$	611.1447	12.8	288314
NAD+	$C_{21}H_{27}N_7O_{14}P_2$	662.1019	8.6	71795
NADH	$C_{21}H_{29}N_7O_{14}P_2$	664.1175	13.9	6960
NADP+	$C_{21}H_{28}N_7O_{17}P_3$	742.0682	13.5	53337
FAD	$C_{27}H_{33}N_9O_{15}P_2$	784.1498	15	65385
acetyl-CoA	$C_{23}H_{38}N_7O_{17}P_3S$	808.1185	15.6	500335

Supplementary Table 4. Parent and product ion formulas and masses, collision energy (CE), retention time (RT), and signal intensity of metabolites measured by the confirmatory LC-triple quadrupole MS/MS analysis.

	parent ion formula	parent m/z	CE (eV)	product ion formula	product m/z	RT (min)	average intensity in samples from glucose-fed cells
fumarate	$C_4H_3O_4^-$	115	11	$C_3H_3O_2^-$	71	30	702
2-keto-isovalerate	$C_5H_7O_3^-$	115	11	$C_4H_7O^-$	71	28	469
Succinate	$C_4H_5O_4^-$	117	10	$C_3H_5O_2^-$	73	23	933
Malate	$C_4H_5O_5^-$	133	12	$C_4H_3O_4^-$	115	26	19384
Hydroxybenzoate	$C_7H_5O_3^-$	137	21	$C_6H_5O^-$	93	22	1845
α-ketoglutarate	$C_5H_5O_5^-$	145	11	$C_4H_5O_3^-$	101	28	5739
orotate	$C_5H_3N_2O_4^-$	155	13	$C_4H_3N_2O_2^-$	111	15	5109
phosphoenolpyruvate	$C_3H_4O_6P^-$	167	20	PO_3^-	79	31	574
DHAP/GAP	$C_3H_6O_6P^-$	169	38	PO_3^-	79	16	1904
glycerol-3-phosphate	$C_3H_8O_6P^-$	171	13	PO_3^-	79	13	797
N-carbamoyl-aspartate	$C_5H_7N_2O_5^-$	175	11	$C_4H_6NO_4^-$	132	26	4842
3-phosphoglycerate/ 2-phosphoglycerate	$C_3H_6O_7P^-$	185	15	$H_2PO_4^-$	97	31	1027
citrate	$C_6H_7O_7^-$	191	13	$C_5H_3O_3^-$	111	32	7440
ribose-5-phosphate	$C_5H_{10}O_8P^-$	229	40	PO_3^-	79	13	622
ribulose-5-phosphate/ xylulose-5-phsophate	$C_5H_{10}O_8P^-$	229	40	PO_3^-	79	14	658
shikimate-3-phosphate	$C_7H_{10}O_8P^-$	253	17	$H_2PO_4^-$	97	12	985
hexose-phosphate	$C_6H_{12}O_9P^-$	259	40	PO_3^-	79	13	6568
6-phospho-D-gluconate	$C_6H_{12}O_{10}P^-$	275	11	$H_2PO_4^-$	97	29	3170
N-acetyl-glucosamine-phosphate	$C_8H_{15}NO_9P^-$	300	32	PO_3^-	79	13	564
cyclic-AMP	$C_{10}H_{11}N_5O_6P^-$	328	31	$C_5H_4N_5^-$	134	29	179
fructose-1,6-bisphosphate	$C_6H_{13}O_{13}P_2^-$	339	28	$H_2PO_4^-$	97	30	10370
trehalose/sucrose	$C_{12}H_{21}O_{11}^-$	341	18	$C_6H_{11}O_6^-$	179	3	1103
UDP-D-glucose	$C_{15}H_{23}N_2O_{17}P_2^-$	565	23	$C_9H_{12}N_2O_9P^-$	323	30	103785
UDP-D-glucuronate	$C_{15}H_{21}N_2O_{18}P_2^-$	579	24	$C_9H_{13}N_2O_{12}P_2^-$	403	34	29960
UDP-acetyl-glucosamine	$C_{17}H_{26}N_3O_{17}P_2^-$	606	26	$C_9H_{11}N_2O_{11}P_2^-$	385	30	18346

Supplementary References

1. Bennett, B.D., Yuan, J., Kimball, E.H. & Rabinowitz, J.D. Absolute quantitation of intracellular metabolite concentrations by an isotope ratio-based approach. *Nature Protocols* **3**, 1299-1311 (2008).
2. Yuan, J., Bennett, B.D. & Rabinowitz, J.D. Kinetic flux profiling for quantitation of cellular metabolic fluxes. *Nat Protoc* **3**, 1328-40 (2008).
3. Gutnick, D., Calvo, J.M., Klopotow.T & Ames, B.N. Compounds Which Serve as Sole Source of Carbon or Nitrogen for Salmonella Typhimurium Lt-2. *Journal of Bacteriology* **100**, 215-219 (1969).
4. Rabinowitz, J.D. & Kimball, E. Acidic acetonitrile for cellular metabolome extraction from Escherichia coli. *Analytical Chemistry* **79**, 6167-6173 (2007).
5. Shevchenko, A., Tomas, H., Havlis, J., Olsen, J.V. & Mann, M. In-gel digestion for mass spectrometric characterization of proteins and proteomes. *Nat Protoc* **1**, 2856-60 (2006).
6. Kitagawa, M. et al. Complete set of ORF clones of Escherichia coli ASKA library (A complete Set of E. coli K-12 ORF archive): Unique resources for biological research. *DNA Research* **12**, 291-299 (2005).
7. Morikawa, M., Izui, K., Taguchi, M. & Katsuki, H. Regulation of Escherichia-Coli Phosphoenolpyruvate Carboxylase by Multiple Effectors Invivo .1. Estimation of the Activities in the Cells Grown on Various Compounds. *Journal of Biochemistry* **87**, 441-449 (1980).
8. Matsuoka, Y. & Shimizu, K. Current status of (13)C-metabolic flux analysis and future perspectives. *Process Biochemistry* **45**, 1873-1881 (2010).
9. Bennett, B.D. et al. Absolute metabolite concentrations and implied enzyme active site occupancy in Escherichia coli. *Nature Chemical Biology* **5**, 593-599 (2009).